Cell Biology
Immunology and Inflammation

Spatial and temporal coordination of Duox/TrpA1/Dh31 and IMD pathways is required for the efficient elimination of pathogenic bacteria in the intestine of *Drosophila* larvae

Reviewed Preprint
v2 • October 22, 2024
Revised by authors

Reviewed Preprint
v1 • June 17, 2024

Fatima Tleiss, Martina Montanari, Romane Milleville, Olivier Pierre, Julien Royet, Dani Osman, Armel Gallet, C Léopold Kurz

Université Côte d'Azur, CNRS, INRAE, ISA, France • Aix-Marseille Université, CNRS, IBDM, Marseille, France • UMR PIMIT (Processus Infectieux en Milieu Insulaire Tropical) CNRS 9192-INSERM 1187-IRD 249-Université de La Réunion, île de La Réunion, France

eLife Assessment

This article describes a novel mechanism allows Drosophila to combat enteric pathogens while also preserving the beneficial indigenous microbiota. The authors provide **compelling** evidence that oral infection of Drosophila larvae by pathogenic bacteria activate a valve that traps the intruders in the anterior midgut, allowing them to be killed by antimicrobial peptides. This is an **important** finding revealing a new mechanism of host defense in the gut of insects.

https://doi.org/10.7554/eLife.98716.2.sa3

Abstract

Multiple gut antimicrobial mechanisms are coordinated in space and time to efficiently fight foodborne pathogens. In *Drosophila melanogaster*, production of reactive oxygen species (ROS) and antimicrobial peptides (AMPs) together with intestinal cell renewal play a key role in eliminating gut microbes. A complementary mechanism would be to isolate and treat pathogenic bacteria while allowing colonization by commensals. Using real-time imaging to follow the fate of ingested bacteria, we demonstrate that while commensal *Lactiplantibacillus plantarum* freely circulate within the intestinal lumen, pathogenic strains such as *Erwinia carotovora* or *Bacillus thuringiensis*, are blocked in the anterior midgut where they are rapidly eliminated by antimicrobial peptides. This sequestration of pathogenic bacteria in the anterior midgut requires the Duox enzyme in enterocytes, and both TrpA1 and Dh31 in enteroendocrine cells. Supplementing larval food with hCGRP, the human homolog of Dh31, is sufficient to block the bacteria, suggesting the existence of a conserved mechanism. While the IMD pathway is essential for eliminating the trapped bacteria, it is dispensable for the blockage. Genetic manipulations impairing bacterial compartmentalization result in

abnormal colonization of posterior midgut regions by pathogenic bacteria. Despite a functional IMD pathway, this ectopic colonization leads to bacterial proliferation and larval death, demonstrating the critical role of bacteria anterior sequestration in larval defense. Our study reveals a temporal orchestration during which pathogenic bacteria, but not innocuous, are confined in the anterior part of the midgut in which they are eliminated in an IMD pathway dependent manner.

Author summary

Typically, when considering the immune response of animals to infection, we focus on classical immunity, encompassing both innate and adaptive aspects such as antimicrobials and circulating immune cells. However, a broader perspective on immunity includes additional strategies that enhance host protection, such as behavioral avoidance and internal mechanisms that restrict pathogen propagation. In our study using *Drosophila* larvae as a model, we uncovered spatially and temporally interconnected events that are crucial for effectively combating intestinal infections. Our findings reveal a two-step defense mechanism: first, the larvae rapidly discriminate between bacterial strains, effectively confining hazardous ones in the anterior section of the intestine. These blocked bacteria trigger the synthesis and release of antimicrobial peptides by the host, which ultimately eradicate the entrapped pathogens. Our experiments show that larvae capable of both limiting bacteria spreading and producing antimicrobial peptides withstand infections. In contrast, the absence of either one of these sequential defenses results in high mortality among the larvae, emphasizing the importance of each step and the necessity of their precise coordination in the immune response.

Introduction

One of the key avenues by which bacterial pathogens infiltrate a host is through the ingestion of contaminated food. Following the entry of bacteria in the intestine, the host defense mechanisms will operate in a temporal manner, with mechanical and constitutive chemical barriers serving as the first line of defense, followed by inducible mechanisms involving the production of reactive oxygen species (ROS), the transcription, translation, and secretion of antimicrobial peptides (AMPs) as well as inter-organ signaling to cope with possible upcoming stages of infection. This temporality is evident between innate and adaptive immunity, with the former considered the primary defense line that contains and combats the threat while preparing the more subtle adaptive response.

To focus on deciphering innate immune processes, the insect *Drosophila melanogaster* has been widely and successfully used (Neyen et al., 2014; Younes et al., 2020). This model has made it possible to establish the chronology of the events involved in the defense against pathogenic bacteria. In *Drosophila,* as in all metazoans, a layer made of mucus, completed with a peritrophic membrane in insect midguts, protects the intestine lining from direct contact with pathogens (Hegedus et al., 2009; Lemaitre and Miguel-Aliaga, 2013; Pelaseyed et al., 2014). In adult *Drosophila*, a conserved immune response involving the production of ROS by Duox (Dual oxidase) enzyme in enterocytes is triggered in the intestine as early as 30 minutes after ingesting pathogenic bacteria. ROS directly damage bacterial membranes (Benguettat et al., 2018; Ha et al., 2009; Ha et al., 2005; Lee et al., 2013) but also exert an indirect effect in adults by triggering visceral spasms through the host detection of ROS mediated by the TrpA1 nociceptor and subsequent secretion of Diuretic Hormone 31 (Dh31) by enteroendocrine cells (Benguettat et al., 2018; Du et al., 2016a). Dh31 then binds its receptor on visceral muscles, triggering contractions that expedite bacterial elimination (Benguettat et al., 2018). This pathway seems to

be conserved during evolution as TrpA1 is a *Drosophila* homolog of TRP receptors that respond to noxious conditions (Ogawa et al., 2016) and Dh31 is the *Drosophila* homolog of the mammalian CGRP (Guo et al., 2021; Nässel and Zandawala, 2019). In parallel, the IMD innate immune pathway is activated following bacterial peptidoglycan detection, leading to the transcription of AMP encoding genes and to the subsequent secretion of the peptides that kill bacteria (Capo et al., 2019).

Previous study has explored the dynamics of food transit involving intestinal valves and Dh31 in the context of *Drosophila* larvae (LaJeunesse et al., 2010). Additionally, the perturbed circulation of bacteria within the intestine has not been documented in the literature though some specific localization of commensal and pathogenic bacteria along the intestine have been observed in insects (Basset et al., 2000; Bosco-Drayon et al., 2012; Lanan et al., 2016; Nardi et al., 2016; Ramond et al., 2021; Yao et al., 2022). However, the intricate interplay between the sequestration of bacteria in specific gut regions and their subsequent elimination has remained unexplored. In our study, we leveraged a novel real-time experimental system designed specifically for *Drosophila* larvae, enabling us to meticulously trace the journey and ultimate fate of pathogenic bacteria ingested alongside food. This approach has allowed us to shed light on the complex mechanisms underpinning bacterial management within the larval gut, contributing a significant advancement to our understanding of host-pathogen interactions at the intestinal level. We characterized a new mechanism implicated in the blockage and elimination of pathogenic bacteria in the anterior part of the midgut. We demonstrated that this confinement is regulated by the ROS/TrpA1/Dh31 axis. Our results delineate a model in which bacterial trapping arises from ROS production in the intestinal lumen in response to pathogenic bacteria. These ROS compounds interact with TrpA1 in Dh31-expressing enteroendocrine cells located between the anterior and middle midgut, leading to Dh31 secretion and subsequent bacterial compartmentalization, suggesting the closure of a valve, a midgut junction structure proposed by (LaJeunesse et al., 2010). Interestingly, we found that we can ectopically induce the trapping of fluorescent particles or innocuous bacteria using human CGRP that replaces Dh31. Our findings also highlight the central role of this blockage, which acts first allowing sufficient time for the subsequent eradication of blocked pathogens by the IMD pathway and its downstream effectors. Collectively, our data unravel a finely tuned coordination between the ROS/TrpA1/Dh31 axis and the IMD pathway, enabling an effective bactericidal action of AMPs.

Results

Bacterial confinement in the anterior part of larval intestine

The translucency of *Drosophila* larvae allows for live studies of immune defense components and their coordination in eradicating pathogenic bacteria. In our prior work, we revealed a modified food transit in larvae exposed to the Gram-negative opportunistic bacterium *Erwinia carotovora carotovora* (*Ecc15*), a process that involved TrpA1 (Keita et al., 2017).

Using blue food dye, we tracked the presence of food in the intestinal lumen and observed that larval guts were blue without bacterial contaminants, while in the presence of *Ecc15*, they appeared clearer (Keita et al., 2017). Such a strategy was already used to delineate whether oral infection by *Pseudomonas entomophila* could modulate food transit (Liehl et al., 2006). However, our previous assay with *Ecc15* was limited to 1h post-ingestion and using a food dye, not directly monitoring the fate of the ingested bacteria over the time. We therefore designed a new protocol allowing to film the fate of fluorescent bacteria once ingested by the larvae. Animals are fed for 1h with food contaminated with fluorescent bacteria to investigate the localization of these pathogens within the intestinal tract. Following this feeding period, the animals were transferred to a wet chamber devoid of food. This setup allowed us to monitor the positional dynamics of the bacteria within the intestine over time, without further food intake influencing the observations. We

principally tested three different fluorescent bacteria: *Ecc15-GFP* (*Ecc*, an opportunistic Gram-negative bacterium), *Bacillus thuringiensis-GFP* (*Bt*, an opportunistic Gram-positive bacterium) and *Lactiplantibacillus plantarum-GFP* (*Lp*, a commensal Gram-positive bacterium). After 1 hour of feeding on contaminated media, *Ecc* and *Bt* were concentrated in the anterior midgut (Movies 1 and 2). The location of the bacteria specifically in the anterior part of the intestine following 1h exposure was confirmed when individuals from populations were imaged and counted (**Fig 1A**). The consistently defined limits of the area containing bacteria in the anterior part of the gut across our observations strongly indicate the presence of a physical boundary. This reproducibility contrasts with what would be expected if the cessation of food intake was responsible for halting bacterial progression, which would likely result in more variable bacterial distributions within the intestine among individual subjects (**Fig 1A**). Remarkably, with animals fed 1h with *Ecc* or *Bt* and transferred in a wet chamber, tracking the GFP signal over time revealed that it remained in the anterior part of the larva and began to fade 6 hours after ingestion (Movies1 and 2; **SUPP1A** and **SUPP1B**). This fading suggests the elimination of the bacteria, while the larva continued to exhibit active movements. This pattern was observed for both *Ecc* and *Bt*. Interestingly, the blockage is reversible and may depend upon the presence or status of the trapped bacteria. Indeed, if fluorescent dextran polymers are co incubated with *Ecc*, both bacteria and dextran are blocked in the anterior part of the intestine and following bacteria-associated fluorescence disappearance, the dextran is released in the posterior part (Movie 3). However, unlike the opportunistic bacteria *Ecc* and *Bt*, a food mixture contaminated with *Lp* led to the bacteria being present in the posterior compartment of the larval midgut after 1 hour of feeding and remained there throughout the 16-hour duration of our observation (Movie 4, **Fig 1A** and **SUPP1C**) (Storelli et al., 2018). To better characterize the blockage phenomenon, we counted the ratio of larvae with trapped GFP-bacteria 1h post feeding. Importantly, in all our experiments, approximately 20% of larvae displayed an absence of fluorescent bacteria within the intestinal lumen. Notably, this proportion remained consistent across different bacterial strains used to contaminate the food, indicating that the specific compartmentalization of pathogenic bacteria we observed is not related to a global food-intake cessation. Instead, these findings suggest the deployment of a targeted sequestration mechanism. Focusing on animals containing fluorescent bacteria, we found that while less than 10% of the larvae had *Lp* blocked in the anterior part of the intestine, more than 80% of the larvae had *Ecc* and *Bt* bacteria localized in the anterior part of the midgut (**Fig 1A** and **1B**). We completed our observation of the posterior location of non-pathogenic bacteria with another harmless species, the OP50 strain of *Escherichia coli* (*Eco*). Less than 20% of the animals fed a mixture containing *Eco* showed a blocking phenotype. The portion of the intestine containing the fluorescent bacteria is delimited posteriorly by an extensive turn, a region that was suggested to act like a valve (LaJeunesse et al., 2010). Importantly, the blockage of pathogenic bacteria (*Ecc* and *Bt*) in the anterior part of the intestine was confirmed using *D. melanogaster* larvae with different genetic backgrounds (**Fig 1C**). To confirm our findings, we dissected the intestines of larvae that had ingested the bacteria. Our analysis confirmed that *Ecc* and *Bt* were predominantly located in the anterior part of the intestines, whereas *Lp* was not, supporting our initial observations (**SUPP2A**). Our data collectively indicate that pathogenic bacteria, such as *Ecc* and *Bt*, are spatially confined to the anterior part of the larval midgut before their disappearance. In contrast, the commensal bacterium *Lp* or the innocuous *Eco* line we used are distributed throughout the midgut, persisting principally in the posterior part.

The anterior intestinal confinement of pathogenic bacteria is dose-specific and occurs rapidly

We hypothesized that the bacterial localization specifically in the anterior part of the larval intestine was an active host response and might be dependent on the bacterial dose. To test this, we exposed larvae to varying concentrations of *Ecc* and *Bt* and measured the blockage ratio. We found that a concentration of 2.10^9 *Ecc* bacteria per ml was sufficient to induce the bacterial compartmentalization, whereas for *Bt*, a concentration of 4.10^{10} *Bt* bacteria per ml was required

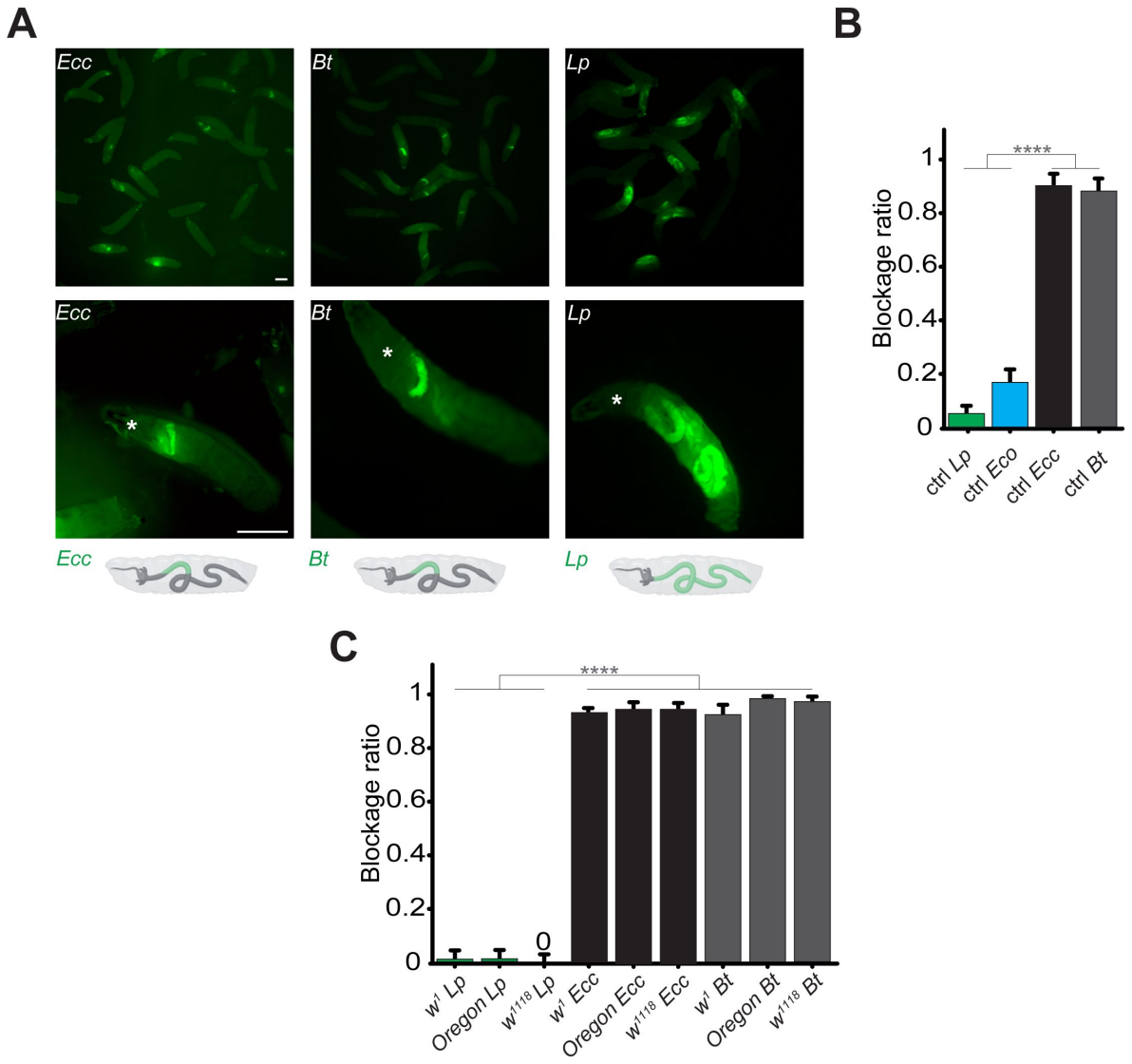

FIGURE 1

Contrary to *Lp or Eco*, *Ecc* or *Bt* bacteria are found exclusively in the anterior part of the gut.

A: Pictures to illustrate the position of the green fluorescence of control (CantonS) L3 stage larvae as a group (upper panel) or individual (lower panel) after having been fed 1h with a media containing yeast and GFP-producing bacteria (*Ecc* or *Bt* or *Lp*). The white asterisk indicates the anterior part of the animal. The white arrow indicates the posterior limit of the area containing the fluorescent bacteria. Below the pictures are schematics representing larvae, their gut, and the relative position of the GFP-producing bacteria in green. Scale bar is 1mm.

B: Graphic representing the blockage ratio for CantonS (ctrl) L3 larvae exposed during 1h to a mixture composed of yeast and fluorescent bacteria: *Lp* or *Escherichia coli* (*Eco*) or *Ecc* or *Bt*. The ratio of control larvae with a distinguishable green fluorescence only in the upper part of the intestine, considered as blocked bacteria, is represented. The ratio is calculated as: x larvae with bacteria exclusively in the anterior part of the gut / (x larvae with bacteria exclusively in the anterior part of the gut + y larvae with bacteria all along the gut). Larvae with no distinguishable fluorescence were considered as non-eaters and discarded from the quantifications. The ratio of larvae with no distinguishable fluorescence was not influenced by the different conditions we tested. Shown is the average blockage ratio with a 95% confidence interval from at least 3 independent assays with at least 30 animals per condition and trial. **** indicates p<0,0001, Fisher exact t-test. See the source data file for details.

C: Blockage ratio for L3 larvae of w^{1}, *Oregon* or w^{1118} isogenized genotypes fed during various times with a mixture combining yeast with *Lp*, *Ecc* or *Bt.* Shown is the average blockage ratio with a 95% confidence interval from at least 3 independent assays with at least 100 animals in total. The 0 symbol indicates an absence of blockage, **** indicates p<0,0001, Fisher exact t-test. See the source data file for details.

(**Fig 2A**). Interestingly, following over time the intoxication of control larvae with a *Bt* concentration of 1.10^{10} bacteria per ml instead of 4.10^{10} *Bt* bacteria per ml revealed that bacteria were not sequestered in the anterior part of the intestine but reached the posterior part (Movie 5). Nonetheless, the fluorescence remained weak likely due to the low amount of bacteria and we could even observed an excretion of bacteria. For all subsequent experiments, we used 4.10^{10} bacteria per ml.

In previous contamination assays, we arbitrary used a 1-hour time point to assess the phenotype. However, observations of bacterial blockage occurring within minutes suggested that this response does not require *de novo* protein synthesis by the host. Shorter exposure times revealed that *Ecc* was blocked in the anterior part of the intestine within 15 minutes, while *Bt* showed a similar pattern beginning at 15 minutes and completing by 30 minutes (**Fig 2B** and **2C**). Based on these results, we defined 1h as our standard exposure time of larvae with bacterial contaminated food. In addition, we performed longer continuous feeding with *Ecc* (20h) to assay whether the blockage would still be present. We observed that while most of the larvae continuously exposed to the contaminated mixture tend to flee and do not contain fluorescent bacteria in their intestine, the ones with detectable fluorescence were blocking the bacteria (**SUPP2B**).

Our assays typically involved groups of approximately 50 larvae to observe population-level phenomena. Recent studies have suggested that larval behavior can be influenced by group dynamics (Dombrovski et al., 2019; Dombrovski et al., 2017; Louis and de Polavieja, 2017; Mast et al., 2014). To determine whether group size affects the bacterial confinement, we exposed groups of varying sizes to *Bt* or *Ecc* and measured the blockage ratio. The phenomenon proved robust even with a single larva exposed to contaminated food, indicating that the response was not influenced by group size under our experimental conditions (**Fig 2D**). Based on these findings, for all subsequent experiments, we standardized the conditions using 4.10^{10} bacteria per ml, a 1-hour exposure time, and groups of at least 20 larvae.

Host TrpA1 and Dh31 are crucial for the blockage phenotype

In our previous study reporting an altered food transit for larvae exposed to a food contaminated with *Ecc* (Keita et al., 2017), we identified the gene *TrpA1* as essential for the host response. The TrpA1 protein, a member of the TRP channel family, facilitates Ca2+ entry into cells at temperatures over 25°C or upon exposure to chemicals such as ROS (Du et al., 2016b; Gu et al., 2019; Guntur et al., 2015). This channel, involved in nociception (Lapointe and Altier, 2011), has been linked to intestinal muscle activity in adult *Drosophila* following *Ecc* exposure (Du et al., 2016a) and in response to ROS production by the host (Benguettat et al., 2018). We examined the role of TrpA1 during the larval response to contaminated food using $TrpA1^{1}$homozygous viable mutant in the experimental setup with fluorescent *Lp*, *Ecc* or *Bt* bacteria. In these mutant larvae, while the localization of *Lp* in the posterior midgut remained unchanged, *Ecc* and *Bt* were found in the posterior midgut following a 1h intoxication and the fluorescence does not fade. (**Fig 3A**, 3B, movie 6 and **SUPP3A**). This observation underscores that TrpA1 is necessary for the blockage of pathogenic bacteria in the anterior midgut and suggests that the disappearance of the fluorescence observed for pathogenic bacteria within the intestine of control animals may be due to bacteria being killed rather than fading of GFP or plasmid loss. Considering previous reports on visceral contraction in adult *Drosophila* linked to ROS production, detection by TrpA1, and Dh31 secretion to expel bacteria (Benguettat et al., 2018; Du et al., 2016a), we wondered whether a similar ROS/TrpA1/Dh31 signaling axis is necessary in larvae to block pathogenic bacteria in the anterior midgut. Indeed, the bacterial blockage we observed might involve muscle contractions related to food contamination. Thus, we tested the blockage ratio of $Dh31^{KG09001}$ homozygous viable mutants exposed to *Lp*, *Bt* or *Ecc* bacteria. In contrast to control animals, where fewer than 20% of larvae exhibited *Ecc* or *Bt* in the posterior section of the intestine, for more than 60% of

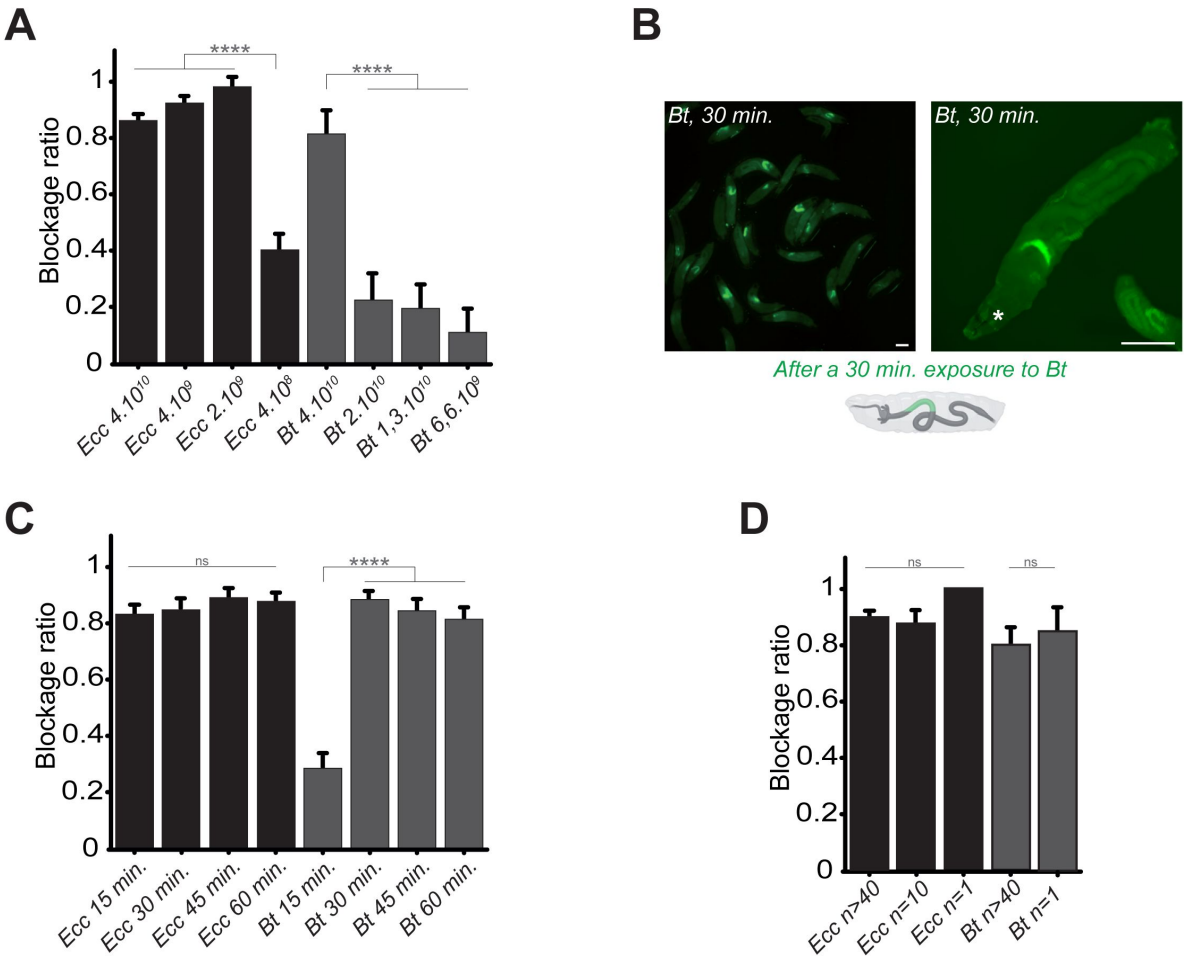

FIGURE 2

Bacterial blockage is dose-dependent, occurs in less than 30 minutes, and does not involve a group effect.

A: Blockage ratio for control L3 larvae fed 1h with a mixture combining yeast with different concentrations of fluorescent *Ecc* or *Bt*, concentrations are in number of bacteria per ml. Shown is the average blockage ratio with a 95% confidence interval from at least 3 independent assays with at least 18 animals per condition and trial. **** indicates p<0,0001, Fisher exact t-test. See the source data file for details.

B: Representative images of control larvae fed during 30 min. with *Bt*. Scale bar is 1mm.

C: Blockage ratio for control L3 larvae fed during various times with a mixture combining yeast with *Ecc* or *Bt.* Shown is the average blockage ratio with a 95% confidence interval from at least 3 independent assays with at least 20 animals per condition and trial. ns indicates values with differences not statistically significant, **** indicates p<0,0001, Fisher exact t-test. See the source data file for details.

D: Blockage ratio for control L3 larvae fed 1h as individual animals or as groups of 10 or >40 with a mixture combining yeast with a constant concentration of *Ecc* or *Bt* (4.10^{10} bacteria per ml). Shown is the average blockage ratio with a 95% confidence interval from at least 3 independent assays with the exact number of animals indicated per condition and trial. ns indicates values with differences not statistically significant, Fischer exact t-test. See the source data file for details.

Dh31^{KG09001} mutant larvae, the pathogenic bacteria *Bt* or *Ecc* were localized in the posterior midgut confirming Dh31's crucial role in this mechanism (**Fig 3A** and **3B**, movie 7 and **SUPP3B**). The localization of *Lp* was not affected (**Fig 3B**).

Given the possibility that the compartmentalization of pathogens we observed might be driven by bacterial virulence factors, we aimed to further investigate the underlying mechanism. To discern whether this phenomenon was specific to pathogenic bacteria or could extend to non-pathogenic entities, we conducted experiments to determine if abiotic particles or non-virulent bacteria could also be ectopically sequestered within the gut. The human Calcitonin Gene-Related Peptide (hCGRP) is the functional homolog of Dh31. Indeed, hCGRP has been shown to promote visceral muscle contractions in adult flies (Benguettat et al., 2018). To investigate whether the bacterial confinement could be triggered without pathogenic bacteria in response to a hormone, we exposed larvae to either *Lp* or Dextran-FITC in the presence of hCGRP. While *Lp* and Dextran-FITC were normally distributed throughout the midgut, adding hCGRP to the food induced a significant blockage (**Fig 3B** and **3C** and movie 8). This observation implies that the confinement of bacteria within the gut is not solely a direct consequence of pathogen toxicity. Intriguingly, despite the larvae being housed in a wet chamber where no further food intake occurs (which could otherwise push the bacteria towards the posterior gut), we noted that *Lp* initially sequestered in the anterior midgut following the administration of hCGRP began to be released in the posterior part after 6 hours (movie 8 and **SUPP3C**). This is suggestive of a dynamic and reversible phenomenon, likely linked to Dh31/hCGRP hormone metabolization. This demonstrates that the process could be triggered independently of the bacteria by a hormone, independently of food-intake *per se*, highlighting it as an active host mechanism that involves a specific portion of the gut capable of limiting the circulation of the bacteria.

Duox in Enterocytes and Dh31 in Pros+ cells control pathogenic bacteria blockage

The activation of TrpA1, potentially leading to the release of Dh31, ((Belinskaia et al., 2023; Kondo et al., 2010; Kunst et al., 2014) could be a consequence of ROS production in the host larval midgut in response to *Ecc* or *Bt*. The larval intestine comprises two main cell populations: enterocytes (ECs) and enteroendocrine cells (EECs). In adult *Drosophila*, Dh31 is stored in EECs and is secreted in response to TrpA1 activation, a process well documented in literature (Benguettat et al., 2018; Chen et al., 2016; Veenstra et al., 2008). The role of ROS in the immunity of adult *Drosophila* intestine following infection has also been reported (Chakrabarti et al., 2012; Ha et al., 2005; Lee et al., 2013; Ryu et al., 2006). To investigate the involvement of ROS in the larval bacterial confinement, we focused on Duox, the primary enzyme responsible for luminal ROS production. We spatially silenced *Duox* expression using RNA interference (*UAS-Duox_IR*) driven by an ubiquitous driver (Da-Gal4), a driver specific of ECs (Mex-Gal4) or Pros-Gal4, a construction driving expression in EECs and subsets of neuroblasts. In parallel, using the same set of drivers, we tested the effects of cell-autonomous *Dh31* silencing using RNAi (*UAS-Dh31_IR*). Upon exposing these larvae to a food mixture contaminated with fluorescent *Ecc* or *Bt*, we assessed the blockage ratio. Our results indicate that in larvae, Duox is essential in ECs for the blockage of both *Ecc* and *Bt* (**Fig 3D**). Furthermore, silencing *Dh31* in EECs not only confirmed the mutant phenotype but also indicated that Dh31, necessary for the confinement, is required for the phenomenon in Pros+ cells. (**Fig 3D**). In order to better delineate the cells required for the phenotype, we specifically silenced *Dh31* in a subset of Dh31+ EECs located at the anterior/acidic midgut junction using the DJ752-Gal4 line, which has been characterized in details in the study by Lajeunesse et al. (2010). Our results demonstrate that upon *Bt* or *Ecc* exposure, the parental DJ752-Gal4 line has a lower capacity to block the bacteria compared to the parental UAS control, but the combination with the *UAS-Dh31-IR* (DJ-Gal4/*UAS-Dh31_IR*) almost totally prevents the blockage phenomenon (**SUPP4**).

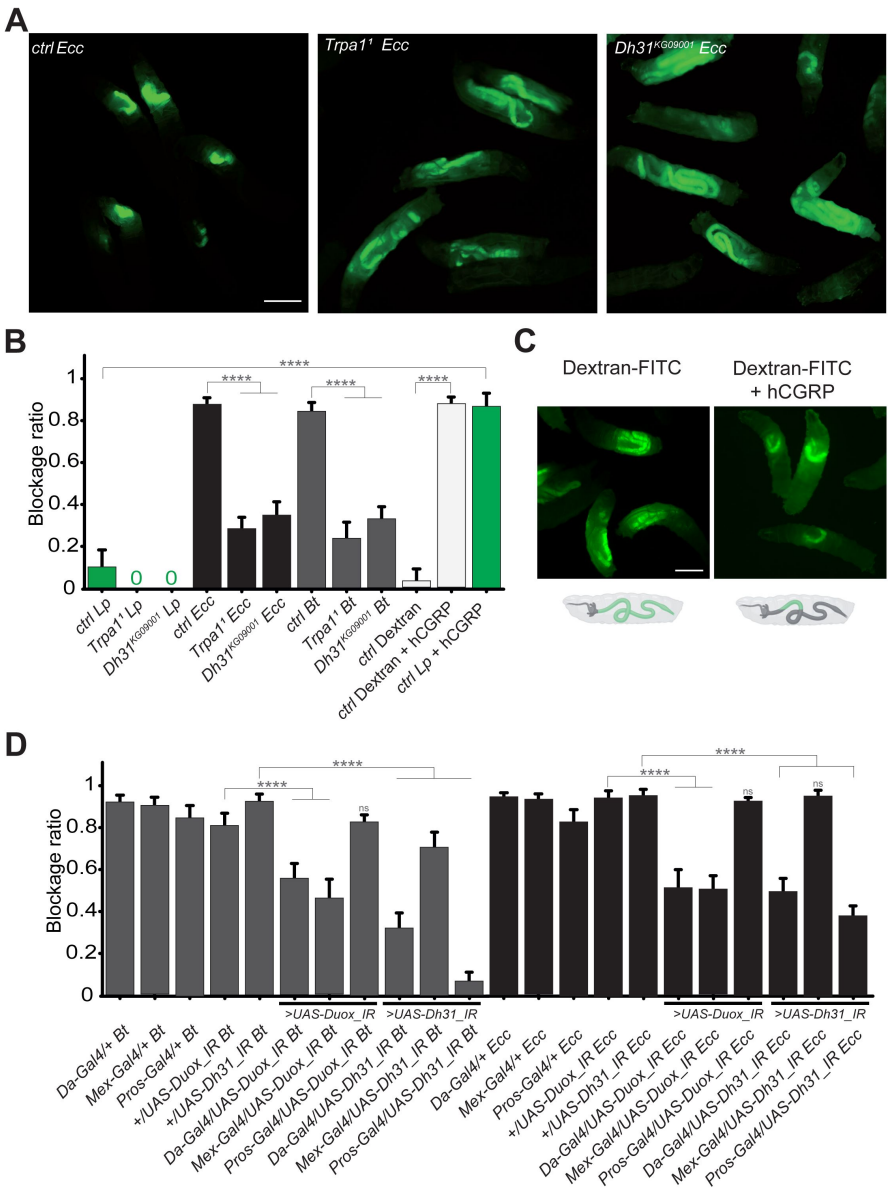

FIGURE 3

The bacterial blockage necessitates Duox in enterocytes, the TrpA1 channel and Dh31 in Pros+ cells.

A: Pictures to illustrate the localization of the fluorescent bacteria within the intestine of control (ctrl), *TrpA1*^{1} or *Dh31*^{KG09001} L3 larvae after having been fed 1h with a mixture of yeast and *Ecc*. Scale bar is 1mm.
B: Blockage ratio for control (ctrl) L3 larvae or mutants for *TrpA1*^{1}or *Dh31*^{KG09001} fed 1h with a mixture combining yeast and *Lp* or *Ecc* or *Bt* or fluorescent Dextran with or without hCGRP hormone. Shown is the average blockage ratio with a 95% confidence interval from at least 3 independent assays with at least 30 animals per condition and trial. 0 indicates an absence of blockage. **** indicates p<0,0001, Fisher exact t-test. See the source data file for details.
C: Pictures to illustrate the localization of the fluorescence within the intestine of control L3 larvae after having been fed 1h with a mixture of yeast and fluorescent Dextran with or without hCGRP hormone. Below the pictures are schematics representing larvae, their gut, and the relative position of the fluorescence in green. Scale bar is 1mm.
D: Blockage ratio for animals expressing RNA interference constructions directed against *Duox* mRNA or *Dh31* mRNA, ubiquitously (Da-Gal4), in enterocytes (Mex-Gal4) or in enteroendocrine cells (Pros-Gal4) and then fed 1h with a mixture combining yeast and *Ecc* or *Bt*. Shown is the average blockage ratio with a 95% confidence interval from at least 3 independent assays with at least 30 animals per condition and trial. ns indicates values with differences not statistically significant, **** indicates p<0,0001, Fisher exact t-test. See the source data file for details.

This data underscores the pivotal roles of Duox in ECs, Dh31 in Pros+ cells and more specifically in the cells expressing the DJ752-Gal4 driver for the entrapment of pathogenic bacteria in the anterior part of the *Drosophila* larval midgut.

Absence of ROS prevents blockage phenotype

Our data demonstrating that Duox protein is necessary for the confinement phenotype, implies that ROS generated by this enzyme are critical. The involvement of TrpA1, a known ROS sensor, further highlights the significance of these compounds in the process. To corroborate the necessity of ROS, we neutralized luminal ROS using DTT (Dithiothreitol), a potent reducing agent known for its efficacy against ROS, mixing it with the larval food (Benguettat et al., 2018). In normal conditions, larvae fed with *Bt* exhibit a compartmentalization of the bacteria in the anterior part of their intestine, as shown previously in FIG 1A, 1B and **Fig 4A**. However, when the larvae were exposed to a mixture of *Bt* and DTT, the intestinal sequestration of bacteria in the anterior midgut was abolished (**Fig 4A**). The effect of DTT over the blockage phenotype was quantified using DTT mixed to Dextran-FITC in order to compare with a condition leading to an almost full posterior localization (FIG 4B).

Evidence that host ROS were the elements that initiated the blocking mechanism raised the question of discrimination between bacteria. Indeed, there are studies linking the chemical signature of pathogens, particularly Uracil, with the release of ROS in the intestinal lumen of adult *Drosophila* (Kim et al., 2020; Lee et al., 2013). *Ecc* and *Bt* are precisely bacteria that release Uracil, unlike *Lp* (Lee et al., 2013). To determine whether it was possible to induce *Lp* blockade by adding Uracil, we used our intoxication protocol supplemented with Uracil. Using an Uracil concentration that was previously demonstrated as sufficient to induce ROS production in adults (Lee et al., 2013), we did not observe the blockage of *Lp* in the anterior part of the intestine (SUPP 5).

Together, our results strongly suggest a discrimination in the larval midgut lumen between commensal and pathogenic bacteria. Such a discrimination involves the Duox enzyme in producing ROS, and these ROS act as key signals initiating the confinement mechanism. ROS may be produced first to directly limit bacterial proliferation but meanwhile trigger a cascade of events leading to sequestration in the anterior part.

Blockage is crucial for bacterial elimination and larval survival

Our real-time observations showed that between 4 and 6 hours after the bacterial compartmentalization of *Bt* or *Ecc* in the anterior midgut, the bacteria disappeared (movies 1 and movie 2, **SUPP1A** and **SUPP1B**). This led us to investigate the relationship between pathogen localization and larval survival. The hypothesis was that the disappearance of the GFP signal corresponded to the bacterial death. We therefore assessed the *Lp*, *Bt* or *Ecc* load over time in dissected midguts of control larvae previously exposed to contaminated food and then transferred to a wet chamber without food. Consistent with our film data, while the *Lp* load remained stable, the quantities of *Ecc* and *Bt* diminished rapidly in the intestines of control larvae by 4h, with no bacteria detectable 8 hours post-ingestion and blockage (**Fig 5A**, **5B** and **5C**). However, in the intestines of $TrpA1^{1}$ and $Dh31^{KG09001}$mutants, and despite a global intestinal immune response comparable to what was measured in control animals (**SUPP6**), the amount of *Bt* and *Ecc* increased overtime (**Fig 5B** and **5C**). Interestingly, the quantity of bacteria presents in the intestine after a 1 hour feeding period was consistent across different host genetic backgrounds for any given bacterial species. This uniformity highlights the process' active regulation rather than attributing the observed patterns to a simple cessation of food intake or a global disruption of peristalsis in *Dh31* and *TrpA1* mutants resulting in a massive and uncontrolled influx of bacteria into the posterior part of the intestine. To verify that the mutants we were using were capable of intestinal muscle movements, we filmed the guts of the $Dh31^{KG09001}$ mutant larvae. We observed strong waves of contractions in the intestines of the $Dh31^{KG09001}$ mutant animals, whether they

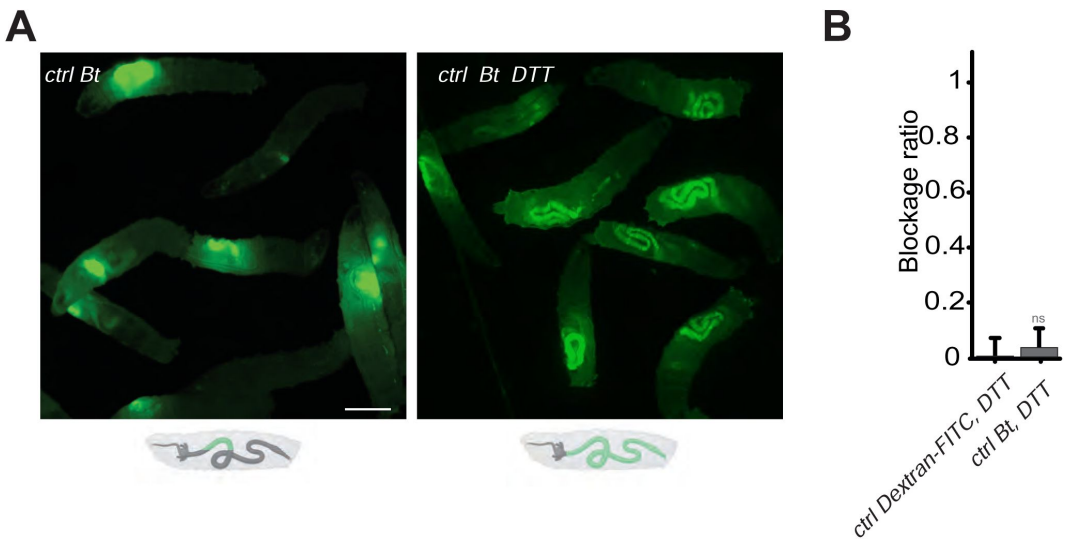

FIGURE 4

Blocking the ROS with DTT prevents the compartmentalization of *Bt*, and the larvae with bacteria in the posterior part of the intestine die.

A: Pictures to illustrate the localization of the fluorescence within the intestine of control (ctrl) L3 larvae after having been fed 1h with a mixture of yeast and *Bt* with or without DTT. Below the pictures are schematics representing larvae, their gut, and the relative position of the fluorescent bacteria in green. Scale bar is 1mm.
B: Blockage ratio for control (ctrl) L3 larvae fed 1h with a mixture combining yeast, DTT and fluorescent Dextran or *Bt*. Shown is the average blockage ratio with a 95% confidence interval from at least 3 independent assays with at least 18 animals per condition and trial. ns indicates values with differences not statistically significant, Fisher exact t-test. See the source data file for details.

were fed with Ecc (movie 9) or not (movie 10). Unfortunately, we were unable to assess the bacterial load in the tested mutants beyond 6 hours due to the deterioration of the midguts. Supporting this, in movies 6 and 7 (**SUPP3A** and **SUPP3B**), we observed that *Bt* or *Ecc* bacteria which were not blocked in the anterior part of the midgut did not disappear over time. More importantly, $TrpA1^{1}$and $Dh31^{KG09001}$ mutant larvae containing *Bt* or *Ecc* stopped to move suggesting they were dead. We confirmed the precocious death of the $TrpA1^{1}$ and $Dh31^{KG09001}$ larvae fed with either *Bt* or *Ecc* compared to control animals (**Fig 5D** and **5E**). Importantly, these mutants exhibited sustained viability overnight in the wet chamber after having been fed 1h with a mixture containing *Lp* or a bacteria-free diet (**Fig 5E**). Interestingly, control larvae fed a mixture of *Bt* and DTT, which neutralizes ROS and thus inhibits the confinement, also perished (**Fig 5F**). This mortality was not due to DTT, as larvae fed Dextran-FITC plus DTT survived (FIG 5F). These findings suggest that, in larvae, the blockage of *Bt* and *Ecc* in the anterior part of the midgut – involving a sequence of events with ROS production by Duox, TrpA1 activation by ROS, and Dh31 secretion – is essential for bacterial elimination by the host. Thus, failure to compartmentalize pathogenic bacteria like *Ecc* or *Bt* results in their proliferation and consequent larval death.

The confined area is delimited by TrpA1+/Dh31+ cells and muscular structures

The above results suggest a working model involving the ROS/TrpA1/Dh31 axis in which Dh31 release from EECs leads to muscle contractions. However, unlike in adult *Drosophila*, where bacteria are expelled from the gut, in larvae, we observed a blockage mechanism. To better understand the physiology of the process, we utilized confocal microscopy to thoroughly examine larval midguts and explore the relationship between TrpA1-positive (TrpA1+) cells, anterior confinement of the bacteria, and muscular structures. In larval midguts, TrpA1+ cells were also Dh31+, and these Dh31+ cells were identified as EECs (Pros+), typically located at the end of the anterior midgut. With the reporter line we used (*TrpA1*-Gal4/UAS-RFP), we noted an average of 3 TrpA1+/Dh31+ cells per gut (ranging from 2 to 6 cells across 14 examined guts, see source data file) (**Fig 6A**-**6F**). Interestingly, these cells may be the ones described previously as being part of a valve (LaJeunesse et al., 2010) and also reported by Zaidman-Rémy and colleagues as being Dh31+ as well as Hml+, an hemocyte marker (Zaidman-Rémy et al., 2012). The identity of these cells was in agreement with our genetic and functional data linking Dh31 with Pros+ cells including EECs (FIG 3D) and suggested that TrpA1 and Dh31 operate within the same cells (**Fig 6C**, 6C' and 6C").

The shape of these TrpA1+ Dh31+ cells was characteristic of EECs (**Fig 6A**'). In agreement with a model involving an interaction of secreted ROS with TrpA1 and a subsequent local Dh31 release to act on muscles, following exposure to food contaminated with fluorescent *Bt* or *Ecc*, the bacteria were confined in an area delimited by the anterior part of the gut and the TrpA1+ cells patch (**Fig 6B**). Additionally, we observed that the amount of Dh31 within Pros+ cells of larvae confining bacteria was lower compared to those not exhibiting the blockage, such as *TrpA1* mutant (**Fig 6D** and **6E**). Then, we wondered whether specific muscle structures would exist close to the TrpA1+ cells in the anterior midgut. Actin labeling revealed fibrous structures on the basal side of the gut and attached to it in a transversal position (**Fig 6C**" and 6F-6H'). These structures, typically lost during dissection, have been described previously, and the hypothesis of their connection with a valve at the junction with the midgut was proposed in a report studying larval midgut peristalsis (LaJeunesse et al., 2010). Notably, the attachment points of these filaments, or tethers, corresponded with the locations of TrpA1+ cells and the boundary of the area where *Ecc* or *Bt* were confined (**Fig 6C**" and 6F-H). These filaments have been described as longitudinal muscles emanating from two out of the four gastric caeca, but this might be a misinterpretation of the images generated by Lajeunesse et al. (2010). Indeed, a recent study describes these muscular structures using *in vivo* observations without dissections. Interestingly, they show that

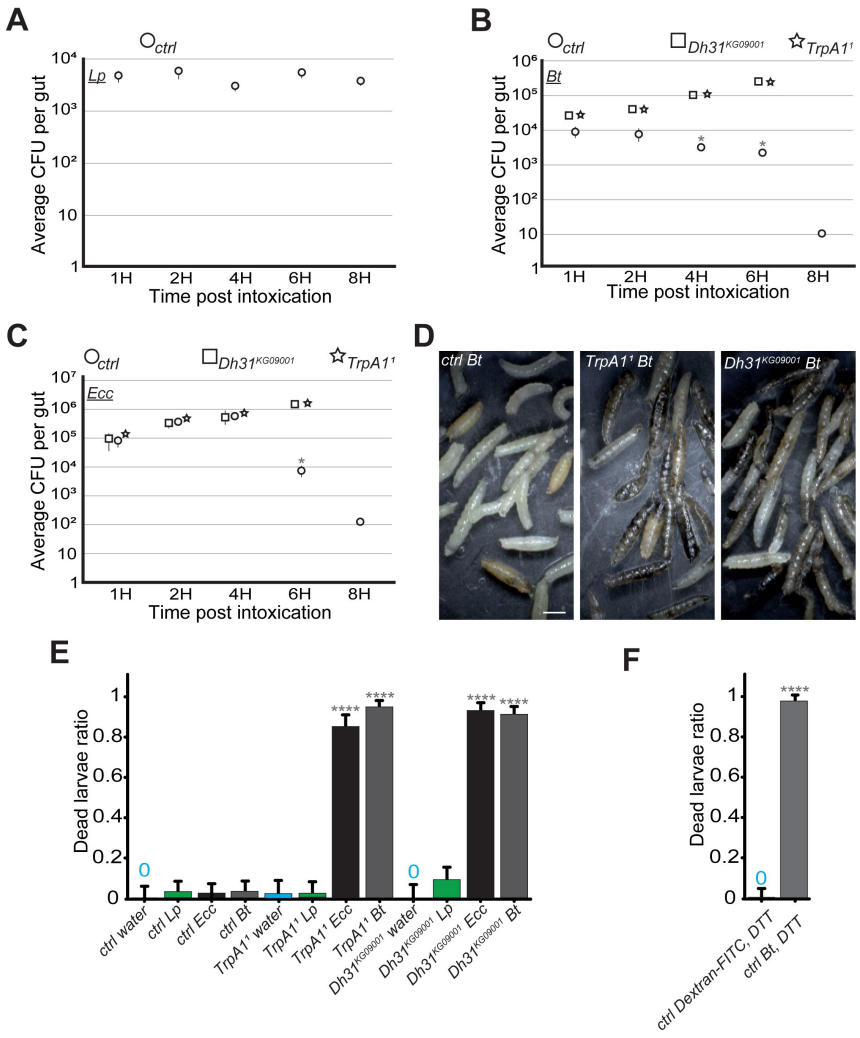

FIGURE 5

In the absence of blockage in *TrpA1*^{1} or *Dh31*^{KG09001} mutants, *Bt* and *Ecc* proliferate in the larval intestine and the larvae die.

A, **B** and **C**: quantification over time of the amount of *Lp*, (A), *Bt* (B) or *Ecc* (C) live bacteria within the larval intestine of control (ctrl) (A, B and C), *Dh31*^{KG09001} (B and C) and *TrpA1*^{1} (B and C) animals following a 1h feeding period with a solution containing yeast and bacteria. CFU stands for Colony Forming Units. Shown is the average ± SEM of at least 3 independent experiments with at least 7 guts each. After 8h, either all the *TrpA1*^{1} or *Dh31*^{KG09001} larvae were dead or the intestines were severely damaged preventing the CFU counting. * Indicates p<0,05, Mann Whitney, two-tailed test. See the source data file for details.

D: Pictures of control (ctrl) or *TrpA1*^{1} or *Dh31*^{KG09001}larvae after 8h in a wet chamber following a 1h feeding with a mixture of yeast and *Bt.* For control larvae, some animals made pupae that are visible while for *TrpA1*^{1} and *Dh31*^{KG09001} mutants, the dark larvae are dead non-moving melanized animals. Scale bar is 1mm.

E: Ratio of dead control or *TrpA1*^{1} or *Dh31*^{KG09001}larvae after 8h in a wet chamber following or not (water) a 1h feeding period with yeast mixed with *Lp* or *Ecc* or *Bt.* Shown is the average with 95% confidence interval of at least 3 independent experiments with at least 21 larvae per trial and condition. The 0 symbol indicates an absence of lethality. **** indicates p<0,0001, Fisher exact t-test. See the source data file for details.

F: Ratio of dead control (ctrl) larvae after 8h in a wet chamber following a 1h feeding period with a mixture combining yeast, DTT and Dextran fluorescent beads or *Bt*.

Shown is the average with 95% confidence interval of at least 3 independent experiments with at least 18 larvae per trial and condition. The 0 symbol indicates an absence of lethality. **** indicates p<0,0001, Fisher exact t-test. See the source data file for details.

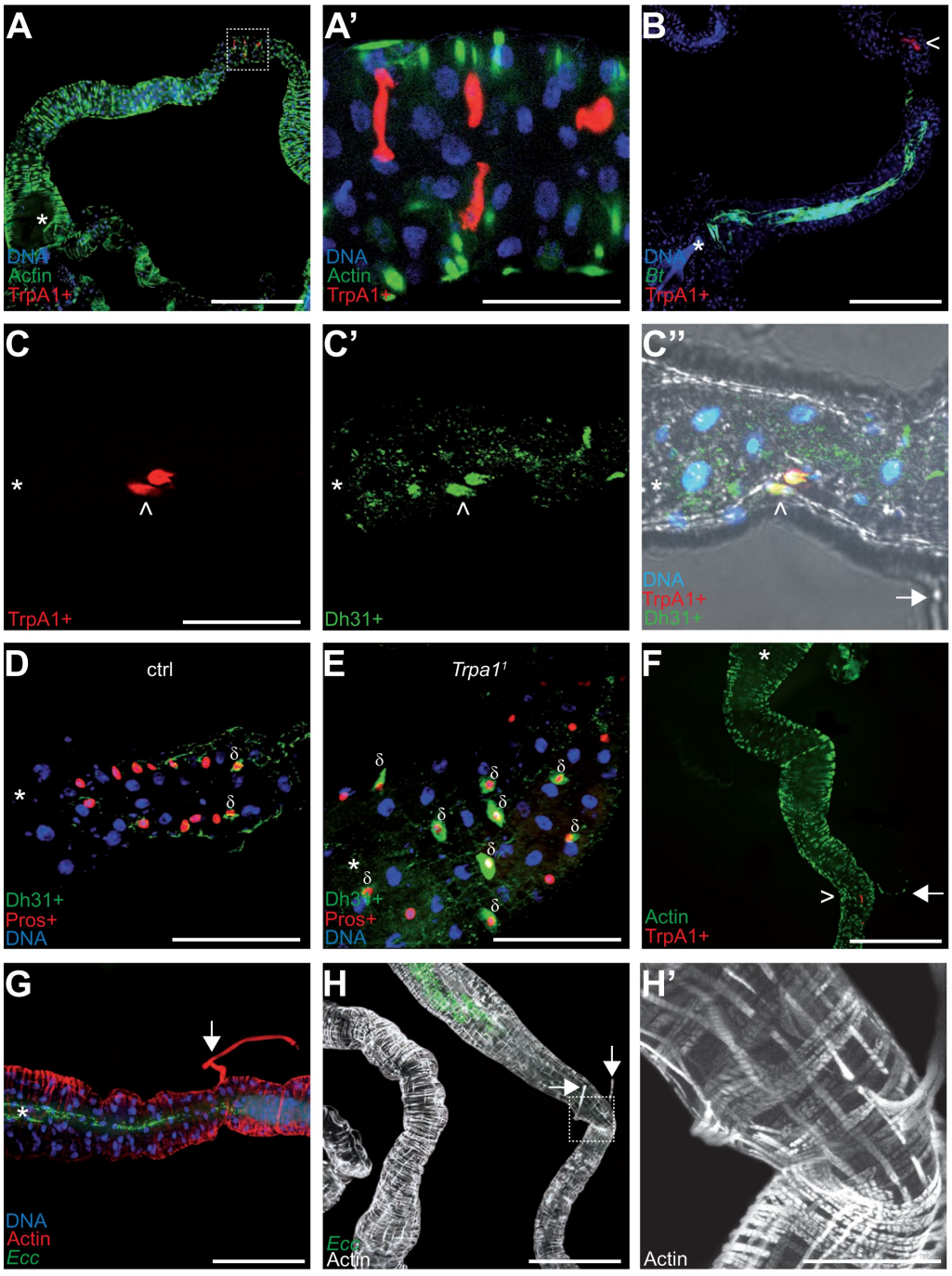

FIGURE 6

TrpA1+ cells in the gut are enteroendocrine cells concentrated in a portion of the intestine bordering the blocked bacteria.

Confocal fluorescent pictures of the anterior portions of L3 larval intestines to detect; longitudinal and transversal muscles concentrated in actin (F, G, H and H'), TrpA1+ cells producing RFP (A, A', B, C, C'' and F), GFP-bacteria (B, G and H), Dh31+ cells (C', C'', D and E), Pros+ cells (D and E) and nuclei with DNA staining (A, A', B, C'', D, E and G).
In B, D, E, G, H and H'; animals were previously fed for 1h with a mixture containing bacteria and yeast with *Bt* (B, D and E) or *Ecc* (G, H and H'). When present, the white star indicates the anterior part of the intestinal portion shown, the arrows point to TARMs and the > symbols point to TrpA1+ cells. The empty squares in A and H with dashed lines correspond to the portion of the image magnified in A' and H', respectively. Scale bar in A, B, F, G and H represents 500µm, in A', C, D, E and H' represents 100 µm.

these muscles belong to a subgroup of alary muscles named TARMs (Thoracic Alary Related Muscles) (Bataillé et al., 2020). Specifically, TARMsT1 connect the anterior of the larvae to the extremities of gastric caeca, while TARMsT2 link the anterior part of the gut to the larval epidermis. Our findings support the hypothesis that the observed muscular structures close to the TrpA1+ cells are TARMsT2 (**Fig 6C**", 6F-6H', **SUPP7** and movie 11). These TARMsT2 are attached to the longitudinal gut muscles and the intestine forms a loop at the attachment site (**Fig 6H**' and **SUPP7**) (Bataillé et al., 2020). The presence of Dh31+ EECs in this specific curved region of the gut close to the TARMsT2 attachment (**Fig 6C**") led to the hypothesis that this region may act like a valve (LaJeunesse et al., 2010). Importantly, we confirmed that these TARMsT2 are still present in $TrpA1^{1}$ and $Dh31^{KG09001}$ larvae (SUPP 8). Our genetic, functional and physiological data confirm the model describing the valve and reveal a new and crucial role in the context of pathogenic bacteria ingestion.

IMD pathway is mandatory for eliminating trapped bacteria

In our study, we observed that control larvae were able to kill *Ecc* and *Bt* bacteria trapped in the anterior part of the gut within 6-8 hours (movies 1 and 2 and **Fig 5A-C**). This finding raised questions about the mechanism of bacterial elimination and the potential role of the IMD (Immune Deficiency) pathway in this process. While larval intestinal immunity is multifaceted, a key defense mechanism against bacteria is the production and secretion of AMPs (Hanson and Lemaitre, 2020). Thus, we focused our investigations on AMPs. Both *Ecc* and *Bt* possess DAP-type peptidoglycans (PGN), known to activate the IMD signaling cascade, which leads to the production of AMPs like Diptericin (Kaneko et al., 2006; Leulier et al., 2003; Stenbak et al., 2004). We used various mutants deficient in components of the IMD pathway, including PGRP-LC and PGRP-LE (PGN receptors), Dredd (an intracellular component), and Relish (a NF-kB transcription factor) (Zhai et al., 2018). Additionally, we studied a mutant, *ΔAMP14*, lacking 14 different AMPs (Carboni et al., 2022). We first assayed whether the IMD pathway was required for the blockage phenotype upon ingestion of *Bt* or *Ecc*. While *Lp* was distributed throughout the gut of IMD pathway mutants, *Ecc* and *Bt* were confined to the anterior part of the intestine, akin to control larvae (movies 12-16, **SUPP9** and **SUPP10** and **Fig 7A** and **7B**). Thus, the IMD pathway is not required for the compartmentalization of *Ecc* and *Bt* in larval intestines. Nevertheless, the movies suggested a death of the IMD mutant larvae despite the blockage of either *Bt* or *Ecc*. We therefore tested the survival of these IMD pathway mutants following a 1h feeding with a mixture containing or not (water) fluorescent bacteria followed by a transfer into a humid chamber. While neither control animals nor the IMD pathway mutants died following a 1h feeding period with a *Lp* contaminated or non-contaminated food and transfer into a humid chamber, all the IMD pathway mutants, including *ΔAMP14*, had a decreased survival after exposure to *Ecc* or *Bt* (**Fig 7C** and **7D**). Thus, the IMD pathway is central for the survival of these animals with bacteria blocked in the anterior part of the intestine. As this increased lethality in IMD pathway mutants might be related to an uncontrolled growth of the confined *Bt* and *Ecc* bacteria, we performed CFU counting. With *Bt* and *Ecc*, while the initial inoculum was divided by 10^{3} in 8h in the control larvae, the bacterial population was maintained and even increased 10-fold in IMD pathway mutants including *ΔAMP14* (**Fig 7E** and **7F**). Additional observations from filming the fate of *Bt* and *Ecc* in IMD pathway mutant larvae confirmed these findings (movies 12-16). The GFP-bacteria, although sequestered in the anterior part of the intestine, did not disappear, coinciding with larval immobility and presumed death. In order to delineate whether the localization of the bacteria within the intestine coincides with the gut area producing the AMPs, we assayed the spatial and temporal activation of the AMP Diptericin-encoding gene (Dpt) using a reporter line intoxicated with fluorescent bacteria. We observed that larvae fed with *Lp* do not robustly express the reporter gene in the posterior part of the intestine, while the bacteria can be seen in this area. Conversely, transgenic animals infected with *Bt* and blocking the bacteria in the anterior part of the gut robustly induce the expression of the AMP-reporter gene in this area (**SUPP11**). In conclusion, our findings illustrate that although the IMD pathway is dispensable for the initial compartmentalization of pathogenic bacteria, a process contingent on the ROS/TrpA1/Dh31 axis, it

plays a crucial role in their subsequent elimination. Indeed, the AMPs produced following IMD pathway activation are essential for killing the trapped bacteria and ensuring larval survival (**Figure 8**).

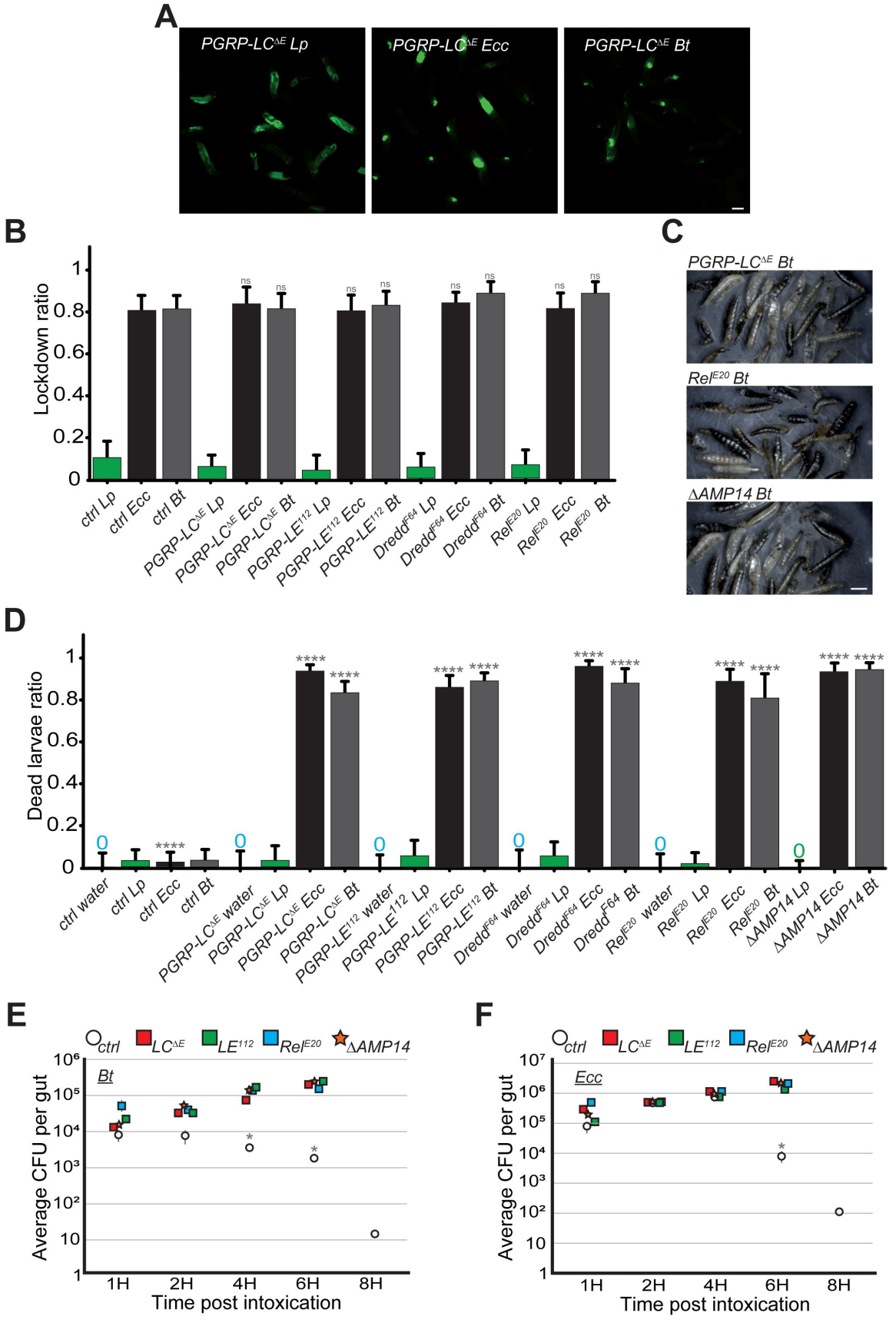
A
PGRP-LC^ΔE Lp
PGRP-LC^ΔE Ecc
PGRP-LC^ΔE Bt
B
Lockdown ratio
ctrl Lp
ctrl Ecc
ctrl Bt
PGRP-LC^ΔE Lp
PGRP-LC^ΔE Ecc
PGRP-LC^ΔE Bt
PGRP-LE^112 Lp
PGRP-LE^112 Ecc
PGRP-LE^112 Bt
Dredd^F64 Lp
Dredd^F64 Ecc
Dredd^F64 Bt
Rel^E20 Lp
Rel^E20 Ecc
Rel^E20 Bt
C
PGRP-LC^ΔE Bt
Rel^E20 Bt
ΔAMP14 Bt
D
Dead larvae ratio
ctrl water
ctrl Lp
ctrl Ecc
ctrl Bt
PGRP-LC^ΔE water
PGRP-LC^ΔE Lp
PGRP-LC^ΔE Ecc
PGRP-LC^ΔE Bt
PGRP-LE^112 water
PGRP-LE^112 Lp
PGRP-LE^112 Ecc
PGRP-LE^112 Bt
Dredd^F64 water
Dredd^F64 Lp
Dredd^F64 Ecc
Dredd^F64 Bt
Rel^E20 water
Rel^E20 Lp
Rel^E20 Ecc
Rel^E20 Bt
ΔAMP14 Lp
ΔAMP14 Ecc
ΔAMP14 Bt
E
ctrl
LC^ΔE
LE^112
Rel^E20
ΔAMP14
Bt
Average CFU per gut
Time post intoxication
1H
2H
4H
6H
8H
F
ctrl
LC^ΔE
LE^112
Rel^E20
ΔAMP14
Ecc
Average CFU per gut
Time post intoxication

FIGURE 7

IMD pathway is not required for the blockage but essential for larvae survival and *Bt* or *Ecc* clearance.

A: Pictures to illustrate the localization of the fluorescence within the intestine of *PGRP-LC*$^{\Delta E}$ L3 larvae after having been fed 1h with a mixture of *Lp* or *Ecc* or *Bt*. Scale bar is 1mm.

B: Blockage ratio for control L3 larvae or mutants of the IMD pathway fed 1h with a mixture combining yeast and *Lp* or *Ecc* or *Bt*. Shown is the average with 95% confidence interval of at least 3 independent experiments with at least 20 larvae per trial and condition. ns indicates values with differences not statistically significant, Fisher exact t-test. See the source data file for details.

C: Pictures of *PGRP-LC*$^{\Delta E}$, *Rel*^{E20} or *ΔAMP14* mutant larvae after 18h in a wet chamber following a 1h feeding with a mixture of yeast and *Bt*. The dark larvae are dead non-moving melanized animals. *ΔAMP14* is a mutant deleted for 14 antimicrobial-encoding genes.

D: Ratio of dead control or *TrpA1*^{1} or *Dh31*^{KG09001}larvae after 18h in a wet chamber following or not (water) a 1h feeding period with yeast mixed with *Lp* or *Ecc* or *Bt.* Shown is the average with 95% confidence interval of at least 3 independent experiments with at least 20 larvae per trial and condition. The 0 symbol indicates an absence of lethality. **** indicates p<0,0001, Fisher exact t-test. See the source data file for details.

E and **F**: quantification over time of the amount of *Bt* (A) and *Ecc* (B) live bacteria within the larval intestine of control or IMD pathway mutant animals including *ΔAMP14* following a 1h feeding period with a solution containing yeast and bacteria. CFU stands for Colony Forming Units. *ΔAMP14* is a mutant deleted for 14 antimicrobial-encoding genes. Shown is the average ± SEM of at least 3 independent experiments with at least 7 guts each. After 8h, either all the mutants were dead or the intestines were severely damaged preventing the CFU counting. * Indicates p<0,05, Mann Whitney, two-tailed test. See the source data file for details.

Discussion

Leveraging the transparency of the *Drosophila* larvae, we have successfully developed a novel real-time experimental system to monitor the fate of fluorescent bacteria ingested along with food. This methodological advancement has enabled us to unveil a previously uncharacterized physiological pathway necessary for the efficacy of the larval intestinal immune response. Our research has uncovered a unique defense mechanism centered around the presumed valve located in the anterior midgut, regulated by the enteroendocrine peptide Dh31 (LaJeunesse et al., 2010). Notably, we observed that the pathogenic bacteria we tested, were confined to the anterior section of the larval intestine as early as 15 minutes post-ingestion. We determined that this intestinal sequestration of pathogenic bacteria necessitates a ROS/TrpA1/Dh31 axis initiated by Duox activity in enterocytes in response to pathogenic bacteria. We suspect the secreted ROS to interact with the TrpA1 ion channel receptor located in Dh31-expressing enteroendocrine cells adjacent to the valve-like structure (**Figure 8**). Previous studies on the interaction between ROS and TrpA1 support our hypothesis (Ogawa et al., 2016). The confining of pathogenic bacteria to the anterior part of the larval intestine is a mandatory step prior to their subsequent elimination by the IMD pathway. Intriguingly, previous studies utilizing fluorescent bacteria have already highlighted a specific localization of pathogenic bacteria in the larval gut. Bacteria such as *Ecc15*, *Pseudomonas entomophila*, *Yersinia pestis*, *Salmonella enterica serovar Typhimurium*, and *Shigella flexneri* were observed predominantly in the anterior part of the larval gut 6 hours after oral infection (Basset et al., 2000; Bosco-Drayon et al., 2012; Earl et al., 2015; Ramond et al., 2021; Vodovar et al., 2005). Our findings suggest that these bacteria can all induce ROS

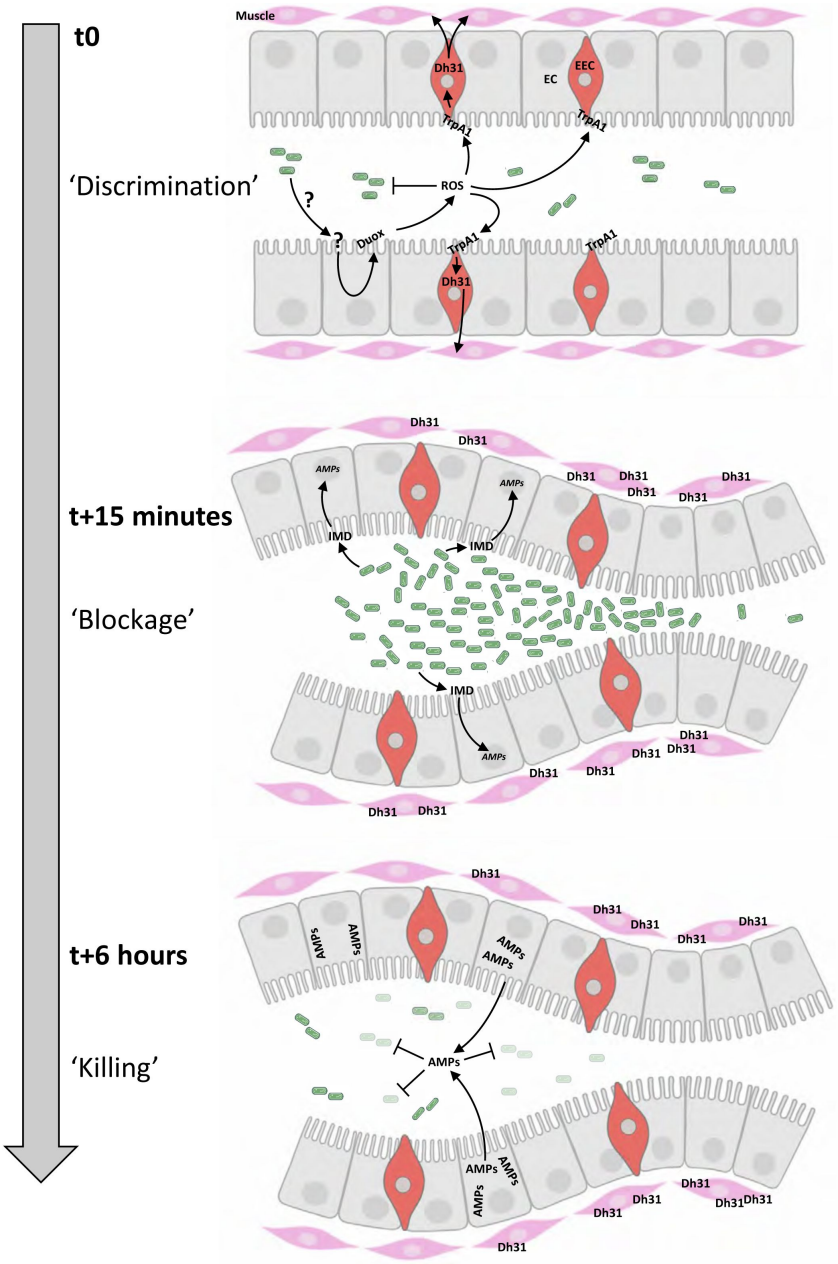

FIGURE 8

Chronological coordination of ROS/TrpA1/Dh31 and IMD pathways for an efficient microbial elimination.

t0: larvae ingest bacteria from the food mixture (anterior on the left, only bacteria similar to *Ecc* or *Bt* are illustrated). This initial phase necessitates a discrimination between commensal and pathogenic bacteria, not elucidated in this study (symbolized by '?'). The presence of pathogenic bacteria induces the production of ROS by enterocytes (EC) in a Duox-dependent manner. Then ROS activates TrpA1 in enteroendocrine cells (EEC). **t15 minutes:** Dh31 secretion by EEC is responsible for the blockage of bacteria likely by promoting visceral muscle contractions leading to a closure of a valve-like structure. This phenomenon concentrates the bacteria in the anterior part of the gut. The bacterial concentration in this part of the intestinal lumen may facilitate the triggering of the IMD signaling cascade that controls the transcription of the genes (*AMPs*) encoding the antimicrobial peptides (AMPs). **t6 hours:** the valve-like structure is still closed. The bactericidal activity of AMPs has eliminated most of the bacteria accumulated in the anterior part of the intestine. Importantly, if confinement is prevented, the larvae die; if the response by antimicrobial peptides is hindered, the larvae die.

production by enterocytes, providing a unifying mechanism for their containment and elimination in the larval gut. Interestingly, it has been reported that the opportunistic pathogen *Staphylococcus aureus (strain USA300)* predominantly colonizes the posterior midgut of *Drosophila* larvae, leading to the death of 93% of the larvae (Ramond et al., 2021). This strain of *S. aureus* produces high levels of detoxifying enzymes, such as catalase and superoxide dismutases, which effectively neutralize ROS. The authors suggested that the neutralization of ROS bactericidal activity by these enzymes is directly responsible for the bacterial proliferation and consequent host mortality (Ramond et al., 2021). However, considering our findings, we propose a complementary or an alternative interpretation: the neutralization of ROS by these detoxifying enzymes might prevent the bacterial compartmentalization, thereby allowing *S. aureus* to access and establish in the posterior midgut. Our data also indicate that when pathogenic bacteria reach the posterior midgut, as observed in larvae fed with DTT or in *TrpA1* or *Dh31* mutants, larval survival is significantly jeopardized. This suggests that larval mortality could be attributed not to the inhibition of ROS in the posterior midgut but rather to the presence of bacteria in this region. In the study by Ramond et al. (2021) involving *S. aureus*, the observation of bacterial spread into the posterior part was recorded 3 hours post-infection. It would be insightful to further investigate the dynamics of bacterial diffusion to determine whether, like other pathogens we studied, *S. aureus* is initially confined to the anterior part of the gut shortly after ingestion, specifically around 15 minutes post-infection. This could provide a broader understanding of the interplay between pathogen-specific strategies and host defense mechanisms in *Drosophila* larvae.

Our study has focused on an elbow-shaped region in the *Drosophila* larval midgut, characterized by a narrowing of the lumen and surrounded by muscular fibers. This region, where we observed a halt in transit when food is contaminated, has been aptly termed a valve due to its functional similarity to the human pyloric region. Interestingly, LaJeunesse et al. (2010) reported the presence of muscular fibers in this area while Bataillé et al. (2020) identified them as a subgroup of alary muscles known as TARMs (Thoracic Alary Related Muscles). Specifically, TARMsT1 connect the anterior part of the larvae to the extremities of a pair of gastric caeca, whereas TARMsT2 link the anterior part of the intestine to the larval epidermis. Our actin staining corroborates the identification of these muscles as TARMsT2, which are attached to the longitudinal muscles of the intestine, causing the intestine to form a loop at the site of attachment (Bataillé et al., 2020). The presence of Dh31-positive enteroendocrine cells (EECs) in this specific elbow-shaped region, close to the TARMsT2 attachment point, combined with our genetic and functional data, supports the hypothesis that this region could exhibit a valve-like activity. This activity is likely triggered by Dh31 or human Calcitonin Gene-Related Peptide (hCGRP) following bacterial exposure. Notably, our previous research in adult *Drosophila* showed that Dh31/hCGRP secretion by EECs induces contractions of the visceral longitudinal muscle fibers, expelling pathogenic bacteria rapidly (Benguettat et al., 2018). However, in larvae, while Dh31/hCGRP likely induces muscle contractions, the ensuing action may manifest as the closure of the midgut junction, as evidenced by the observed retention of pathogenic bacteria. Importantly, in both larvae and adults, the same pathway and type of muscle fibers appear to be involved, as TARMsT2 are connected to longitudinal fibers (**Figure 6H**') (LaJeunesse et al., 2010). This finding is significant as it illustrates a conserved mechanism across developmental stages, albeit with different outcomes: expulsion of pathogens in adults and containment in larvae. In both cases, the overarching objective is the effective elimination of pathogens, demonstrating the versatility and adaptability of the *Drosophila* immune response.

Hence, our work shed lights on a yet to be anatomically characterized valve structure within the *Drosophila* larval gut, presenting a potential model for studying the functions and roles of mammalian pylori. Notably, CGRP (Calcitonin Gene-Related Peptide) secreting enteroendocrine cells have been identified in the mammalian pylorus, as highlighted in research by (Kasacka, 2009) and (Bulc et al., 2018). Drawing parallels with mammalian stomachs, the pylorus is typically closed, opening only when the stomach becomes full. In exploring the functionality of the *Drosophila* valve we studied, we considered two hypotheses: one, where it operates similarly to its

mammalian counterpart, closing by default and opening in response to a full stomach, and another, where it remains open by default and closes upon detection of infected food in the intestine. Our observations with the commensal bacteria *Lp* (movie 4) suggest an initial closure of the pylorus as food accumulates in the anterior part of the intestine, followed by its opening to allow the passage of non-pathogen-contaminated food. This indicates a dynamic and responsive mechanism in the *Drosophila* gut. In contrast, when *Drosophila* larvae encounter food contaminated with pathogenic bacteria, the valve seems to contract, effectively blocking the passage of contaminated food into the anterior part of the intestine. This finding is significant as it not only reveals a unique physiological response in *Drosophila* larvae but also provides a basis for comparative studies with the mammalian gastrointestinal system, particularly in understanding the regulatory mechanisms governing pyloric function.

An intriguing question is why animals without a functional IMD pathway die from *Ecc* or *Bt* exposure while ROS production is still operating? Indeed, when the IMD pathway is disabled, bacteria are still confined in the anterior part of the gut, but are not effectively eliminated, resulting in larval death. This outcome strongly suggests that ROS alone are insufficient for bacterial eradication, even though they have been shown to damage and inhibit bacterial proliferation (Benguettat et al., 2018; Ha et al., 2005). However, the role of ROS in the immune response remains crucial since their timing of expression before antimicrobial peptides is likely a key factor for the efficiency of the immune response. Our findings, together with those from other studies, highlight the critical role of AMPs in fighting off virulent intestinal bacteria, particularly in scenarios where ROS activity is compromised or inadequate (Ramond et al., 2021; Ryu et al., 2006). Our findings emphasize the critical role of the ROS/TrpA1/Dh31 axis in effectively eradicating ingested pathogens. The rapid production of ROS following bacterial ingestion plays a pivotal role in closing the valve and retaining virulent bacteria in the anterior midgut. Notably, this process does not necessitate a transcriptional/translation response. In contrast, the production of antimicrobial peptides is a lengthier process, involving the transcriptional activation of *AMP* genes downstream of the IMD pathway, followed by their translation and secretion. The initial confinement of bacteria in the anterior midgut allows time for AMPs to be produced to eliminate the trapped bacteria, which is crucial for the organismal survival. This anterior bacterial blockage is important since when virulent bacteria reach the posterior midgut (in absence of ROS or in *TrpA1* or *Dh31* mutants) the larvae die despite a functional IMD pathway. A key question arises: Is the posterior midgut less equipped to combat bacteria? Interestingly, it has been previously shown in both *Drosophila* larvae and adults that while the posterior midgut can produce AMPs, it is predominantly dedicated to dampening the immune response, particularly through the production of amidases and the activity of the transcription factor Caudal, both that repressing AMP gene expression (Bosco-Drayon et al., 2012; Hachfi et al., 2024; Ryu et al., 2008). This permits an immune tolerance likely fostering the establishment of the commensal flora. Consistent with this, we observed that commensal bacteria like *Lp* transit from the anterior to the posterior midgut and persist there without compromising larval survival. Additionally, *Lp* inherent resistance to AMPs (Arias-Rojas et al., 2023) further underscores the idea that the anterior midgut serves as a checkpoint where certain bacteria are detained and eliminated, while others, like *Lp*, are permitted to pass through. When the compartmentalization mechanism is compromised, pathogens or pathobionts can spread into the posterior midgut, potentially eliciting an inadequate dampened immune response. Thus, the anterior midgut acts as a critical juncture in determining the fate of ingested bacteria, either leading to their elimination or allowing their passage to the posterior midgut, where a more tolerant immune environment prevails.

Understanding the practical application of this defense mechanism in the natural environment of *Drosophila melanogaster* larvae is crucial. In the wild, *Drosophila* adults are typically drawn to rotting fruits on which they lay eggs, exposing them and their progeny to a plethora of fungi and bacteria. Consequently, developing larvae feed and grow in these non-sterile conditions. In such environments, encountering pathogenic microbes is inevitable. Evasion or avoidance behavior has been documented as a potential strategy for dealing with pathogens (Surendran et al., 2017).

This behavior might enable larvae to seek environments that will supposedly better sustain their survival. However, given the larvae constant consumption of their surrounding media in a race to reach pupation, ingestion of pathogen-contaminated food is a common risk. Under these circumstances, larvae have limited options prior to the activation of their innate immune response. Discriminating innocuous from potentially deleterious bacteria and then limiting the transit of the latter ones for subsequent elimination by AMPs, clearly benefits the host. Nonetheless, the effectiveness of this blockage strategy would be maximized if it were coordinated with evasion behaviors. Such coordination could prevent repeated engagement in this energy-intensive immune response, thus optimizing the larvae chances of reaching pupation successfully. In this context, it is interesting to note that the ROS/TrpA1/Dh31 axis is shared between larvae and adults to manage bacterial infection, but larvae block and kill the pathogens while adults eject them. If larvae eject their gut content, they may ingest it within minutes while adults can fly to another fruit within seconds. This interplay between immune response and behavioral adaptation underlines the sophisticated strategies employed by *Drosophila* larvae to navigate their microbial-rich environment.

Materials and methods

1 Bacterial strain

We used the following strains: *Bacillus-thuringiensis*-GFP (*Bt*) (Hachfi et al., 2024) (the original strain, 4D22, is from the Bacillus Genetics Stock Center - *www.bgsc.org*), *Erwinia carotovora* subsp. *carotovora*-GFP *15* (*Ecc*) (Basset et al., 2000), *Escherichia coli* strain OP50-GFP (a slow growing and innocuous strain used to feed nematodes; *Eco*) (gift from Jonathan Ewbank) and *Lactiplantibacillus plantarum*-GFP (*Lp*) (gift from Renata Matos and François Leulier) (Storelli et al., 2018). *Eco*, *Bt* and *Ecc* were grown on standard LB agar plates at 37°C (*Eco*) or 30°C (*Bt*, *Ecc*) and *Lp* was grown in MRS medium in anaerobic conditions at 37°C for at least 18 hours. Importantly, we used vegetative cells of *Bt* without Cry toxins. Cry toxins are only produced during sporulation and are enclosed in a crystal within the spore. The *Bt* strain we used is 4D22 which have been deleted for the plasmids encoding for the Cry toxins. So, there is no Cry toxin in the *Bt*-GFP vegetative cells we used.

The solid medium used in our experiments was supplemented with antibiotics to ensure the selective growth of our bacterial strains as follows: *Ecc*: Spectinomycin at 100µg/ml; *Bt*: Erythromycin at 10µg/ml; *Lp*: Chloramphenicol at 10µg/ml. Each bacterium was plated from glycerol stocks for each experiment. A single colony was used to prepare liquid cultures. Bacteria were inoculated in 500 ml of appropriate medium containing antibiotics as follows *Ecc*: Spectinomycin at 100 µg/ml; *Bt*: Erythromycin at 10µg/ml; *Lp*: Chloramphenicol at 10µg/ml. After overnight growth, the cultures were centrifuged for 15 min at 7500 rpm. Bacterial infectious doses were adjusted by measuring culture turbidity at an optical density of 600 nm. OD_{600}=100 for *Eco*, Lp and *Ecc* corresponds to $4.9.10^7$CFU/µl. OD_{600}=100 for *Bt* corresponds to $1,5.10^7$CFU/µl.

2 FLY Stocks

Flies were maintained at 25 °C on our standard fly medium (Nawrot-Esposito et al., 2020) with12:12 light/dark cycle. Fly stocks used in this study and their origins are as follows: Canton S (Bloomington #64349, the reference to compare with mutants and noted as control), w^{1118} (Bloomington #5905), w^{1} (Bloomington #145), *Oregon* (Bloomington #5), $TrpA1^{1}$ (Bloomington #26504), $Dh31^{KG09001}$ (Bloomington #16474), *Dh31-Gal4* (Bloomington #51988), $PGRP\text{-}LC^{\Delta E}$ (Bloomington #55713), $PGRP\text{-}LE^{112}$(Bloomington #33055), $Dredd^{F64}$ (Gift from B. Charroux), $Relish^{E20}$(Bloomington #55714), DJ752-Gal4 (Bloomington #8182), *ΔAMP14* (Gift from B. Lemaitre; (Carboni et al., 2022)), *yw*;;*Dpt-Cherry* (Gift from B. Charroux), *TrpA1*-Gal4/UAS-RFP (Gal4 is

Bloomington #527593, UAS is Bloomington #27392), *Da*-Gal4 (Bloomington #55851), *Pros*-Gal4 (gift form B. Charroux), *Mex*-Gal4 (gift from B. Charroux), UAS-*Duox _IR* (Bloomington #38907), UAS-*Dh31_IR* (Bloomington#25925).

3 Infection experiments

Oral infections were performed on mid-L3 larvae (3.5 days after egg laying). For each experiment, between 20 and 50 non-wandering L3 larvae raised at 25°C were collected and washed in PBS (1x). Bacterial pellets with starting OD 600nm ranging from 300 to 400 were aligned with PBS1x at twice the desired final concentration. Then, they were mixed 1:1 with yeast 40% in PBS (1x) and 500 µl of the infected food were added at the bottom of an empty plastic fly vial (VWR) before adding the larvae and sealing it with Parafilm. Then, the larvae were placed at 25°C in the dark. After 60 min, the larvae were washed in PBS (1x) and then counted for the presence of GFP-bacteria or for other analyses. For experiments involving fluorescent Dextran, 1.25mg/mL of Dextran 4kDa (Sigma ref 46944 for FITC-coupled and ref T1037 for TRITC-coupled) was added to the feeding medium. For experiments involving Uracil supplementation, Uracil (SIGMA U0750-5G) was added at 20nM final to the feeding mixture containing *Lp*.

4 Larvae dissection

After 60 min, the infected larvae were washed in PBS (1x). Guts were dissected and fixed in formaldehyde 4% for 45 min, then washed twice in PBS (1x) for 10 min. Guts were mounted between poly-L-lysine (SIGMA P8920-100ML) coated slides and coverslips in Vectashield/DAPI (Vector Laboratories).

5 Colony-forming unit (CFU) counting

Following the established protocol for infection experiments, animals were exposed to contaminated food for 1 hour. Subsequently, animals that had ingested bacteria were either immediately processed for the initial time-point analysis or transferred to a wet chamber for assessment at subsequent time-points. Importantly, since there was no further exposure to contaminated food beyond the 1-hour treatment period, the CFU assays we conducted measured the changes in the initial bacterial load within the larvae over time. Infected animals were washed in ethanol 70% for 30s then rinsed in PBS (1x). Guts were dissected in PBS (1x) and homogenized with a micropestle in 200 µl of LB medium. Samples were serially diluted in LB medium and plated on LB agar plates overnight at 30°C. The Colonies Forming Unit (CFU) were counted the following day. CFU counting has been performed at 5 time points: 1h, 2h, 4h, 6h and 8h after a 60 min intoxication (at least 20 larvae per point and 3 independent repeats).

6 Mortality test

Oral infection of the larvae was performed as described above in *Infection experiments*. Larvae of the different genotypes fed 1h with *Bt*, *Lp* or *Ecc* were quickly washed in 70% ethanol and then PBS (1x). Only the larvae that have eaten (containing GFP bacteria in their intestine) were selected and put in a wet chamber for 18h at 25°C. Mortality was evaluated at this time-point.

7 DTT and CGRP feeding

Oral infection of the larvae was performed as described above in *Infection experiments*.

DTT: DTT was added to the food at a final concentration of 100 nM and larvae were fed during 60 min.

hCGRP: hCGRP (Sigma #C0167) was resuspended in distilled water. Larvae were fed 1h as described above with a final hCGRP concentration of 400 µg/ml.

8 Immunostaining

Dissected intestines were washed twice with PBS (1x)-0.1% Triton X100 then incubated for 3h in the blocking solution (10% of fetal calf serum, 0.1% Triton X100, PBS (1x)). The blocking solution was removed and the primary antibodies added and incubated overnight à 4°C in blocking solution. The following antibodies were used: mouse anti-Prospero (MR1A-c, Developmental Studies Hybridoma Bank (DSHB)) at 1:200 and rabbit anti-Dh31 (gift from Jan Veenstra and Michael Nitabach; (Kunst et al., 2014; Park et al., 2008) at 1:500. Secondary antibodies used were anti-mouse Alexa647 (Invitrogen Cat# A-21235), anti-rabbit Alexa546 (Invitrogen Cat# A-11010). All secondary antibodies were used at 1:1000. Guts were mounted in Fluoroshield-DAPI mounting medium (Sigma F6057). Observations of GFP producing bacteria and of TRPA1+ cells were done using the native fluorescence without immunostaining. For microscopy involving actin staining, fluorescent phalloidin (Sigma P5282, 1/100) was added following the above protocol as if it was the primary antibody, but with a 10 minutes incubation time.

9 RNAi experiments

All the tested animals were F1 obtained from a cross between parents possessing the Gal4 transgene and parents possessing the UAS-RNAi construction or from crosses between w-animals (genetic background of the Gal4 and UAS lines) and a transgenic line to serve as ctrl. The larvae were then fed with contaminated food as described above.

10 RT-qPCR

Oral infection of the larvae was performed as described above in *Infection experiments*. Larvae of the different genotypes fed 1h with *Bt*, *Lp*, *Ecc* or yeast only were quickly washed in 70% ethanol and then PBS (1x). Only the larvae that have eaten (containing GFP bacteria in their intestine, except for the yeast only condition) were selected and put in a wet chamber in the dark for 5h at 25°C. RNA from larval guts (n = 10 for each test and condition) was extracted with RNeasy Mini Kit (QIAGEN, cat. #74106). Quantitative real-time PCR, TaqMan, and SYBR Green analysis were performed as previously described in Charroux *et al.*, 2018. The amount of mRNA detected was normalized to control rp49 mRNA values. Normalized data was used to quantify the relative levels of a given mRNA according to cycling threshold analysis (ΔCt). Control and experimental conditions were tested in the same 'run'. Each sample was normalized to its own rp49 control to take into account age-specific changes in gene expression. Results are presented as average and standard deviation of arbitrary CT of the tested gene from a minimum of three independent experiments. See the source data file for details. Primers used for RT-qPCR are:

rp49: GACGCTTCAAGGGACAGTATCTG, AAACGCGGTTCTGCATGA

Diptericin: GCTGCGCAATCGCTTCTACT, TGGTGGAGTGGGCTTCATG

Attacin D: GTCACTAGGGTTCCTCAG, GCCGAAATCGGACTTG

Drosomycin: CGTGAGAACCTTTTCCAATATGATG, TTCCACGACCACCAGCAT

11 Images and movie acquisition

Images acquisition was performed at the microscopy platform of the Institut Sophia Agrobiotech (INRAE 1355-UCA-CNRS 7254-Sophia Antipolis) with the macroscope Zeiss AxioZoom V16 with an Apotome 2 or a Zeiss Axioplan Z1 with Apotome 2 microscope. Images were analyzed using ZEN and Photoshop softwares. Movie acquisitions were performed with the macroscope Zeiss AxioZoom V16 equipped with the Hamamatsu Flash 4LT Camera. Larvae were captured every 5 minutes. Dead larva images were acquired with a numeric Keyence VHX 2000 microscope.

12 Data representation and statistical analyses

The Graphpad Prism 8 software was used for statistical analyses.

CFU data analysis: the D'Agostino–Pearson test to assay whether the values are distributed normally was applied. As not all the data sets were considered normal, non-parametric statistical analysis such as non-parametric unpaired Mann–Whitney two-tailed tests was used for all the data presented.

Blockage ratio and survival ratio datasets: as the values obtained from one larva are categorical data with a *Yes* or *No* value, we used the two-sided Fisher exact t-test and the 95% confidence interval to test the statistical significance of a possible difference between a test sample and the related control.

For all the quantitative assays, at least 3 independent experiments were performed and some were done in two different laboratories by more than one experimenter. The results from all the experiments were gathered and the total amount of larvae tested is indicated in the source data file. In addition, we do not show the average response from one experiment representative of the different biological replicates, but an average from all the data generated during the independent experiments in one graph.

13 Source data files: detailed lines, conditions and statistics for the figure section

A file containing raw data, all the details about the experiments including the replicates, sample size, genotypes and detailed statistical analyzes is available *https://figshare.com/articles/dataset/Tleiss_et_al_lockdown_Source_Data_File/2501* 8352

DOI: 10.6084/m9.figshare.25018352

Movies

Movie 1

https://doi.org/10.6084/m9.figshare.25018385.v2

DOI: 10.6084/m9.figshare.25018385

Fluorescent *Ecc* is blocked in the anterior part of the larval intestine then vanishes.

Live imaging during 12h of a L3 control larva previously fed 1h with a food containing

Ecc fluorescent bacteria then transferred on a glass slide in a wet chamber.

Movie 2

https://doi.org/10.6084/m9.figshare.25018427.v2

DOI: 10.6084/m9.figshare.25018427

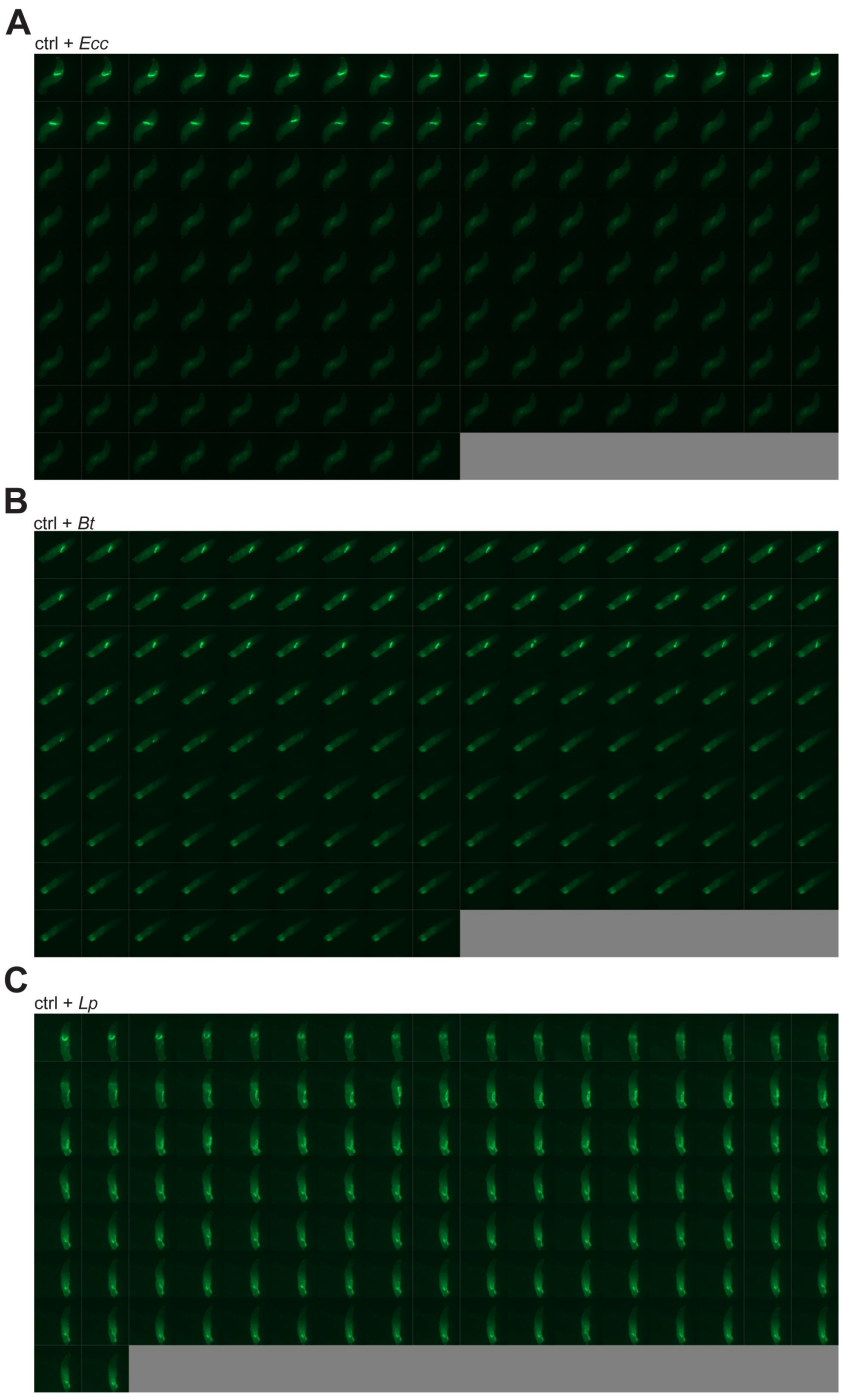

SUPP1

Ecc and *Bt* are blocked in the anterior part of the intestine and disappear while *Lp* transits to the posterior part and remains.

A: Timelapse from the movies of L3 Larvae fed 1h with a mixture of yeast and *Ecc* then transferred on a glass slide, in a wet chamber, to be imaged overnight. Refers to Movie 1.
B: Timelapse from the movies of L3 Larvae fed 1h with a mixture of yeast and *Bt* then transferred on a glass slide, in a wet chamber, to be imaged overnight. Refers to Movie 2.
C: Timelapse from the movies of L3 Larvae fed 1h with a mixture of yeast and *Lp* then transferred on a glass slide, in a wet chamber, to be imaged overnight. Refers to Movie 3.
For A-C, the frames are separated by 5 minutes.

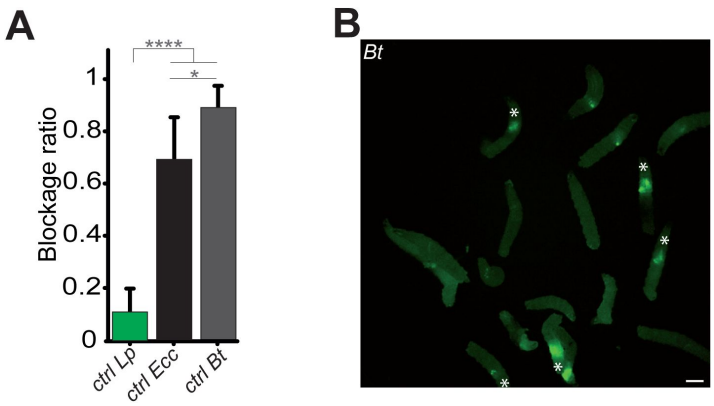

SUPP2

Contrary to *Lp*, *Ecc* or *Bt* bacteria are blocked in the anterior part of the gut.

A: Graphic representing the blockage ratio for dissected intestines of L3 larvae exposed during 1h to a mixture composed of yeast and fluorescent bacteria. Shown is the average blockage ratio with a 95% confidence interval from at least 3 independent assays with at least 8 organs per condition and trial. **** indicates p<0,0001, Fisher exact t-test. See the source data file for details.
B: Picture to illustrate the position of the green fluorescence of control (CantonS) L3 stage larvae as a group after having been fed 20h with a media containing yeast and GFP-*Bt*. The white asterisk indicates the anterior part of the animals. Scale bar is 1mm.

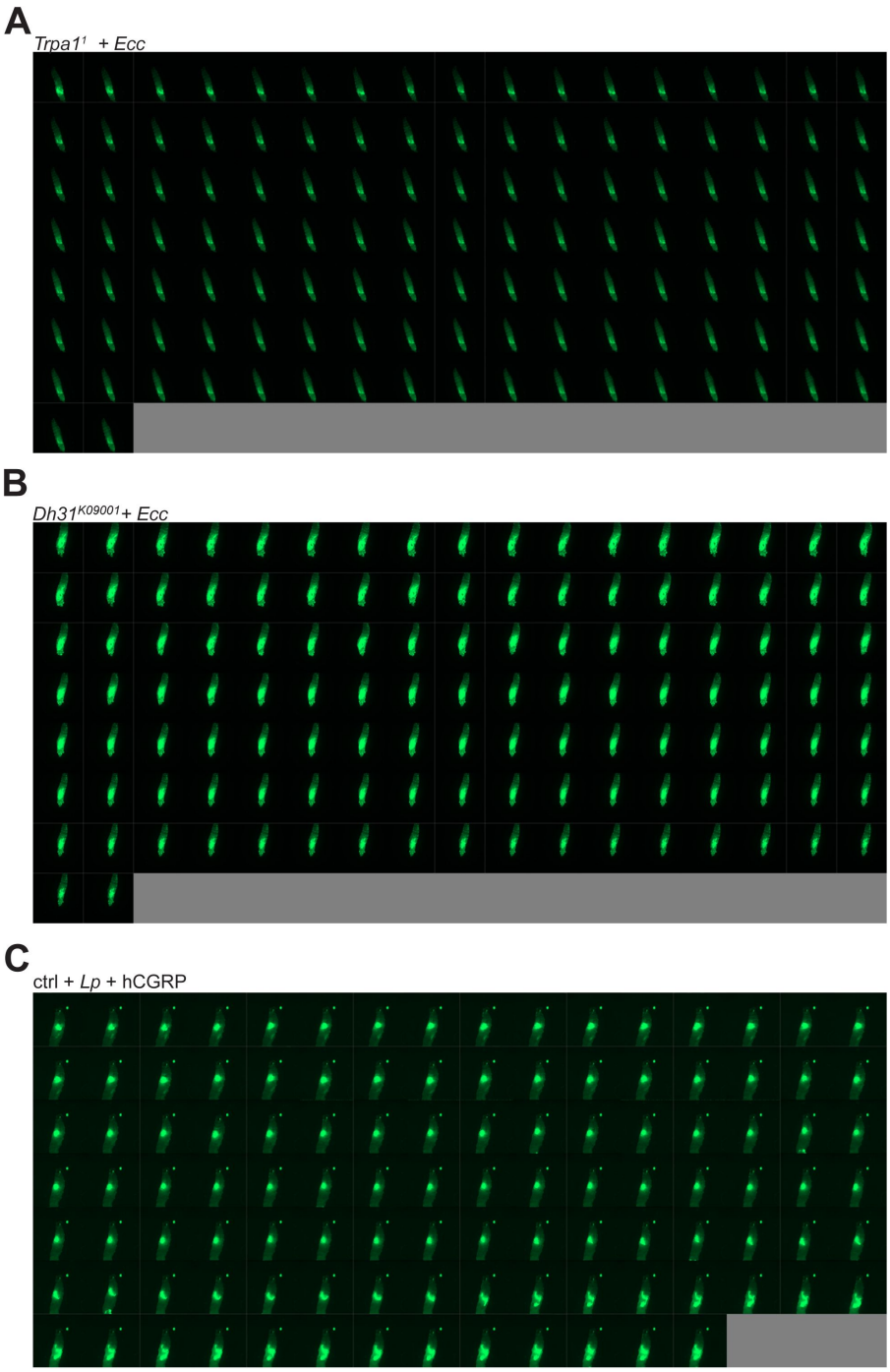

SUPP3

Ecc is not blocked anteriorly in *TrpA1*^{1} and *Dh31*^{KG09001} mutants, persists in the posterior part of the intestine and disappears while *Lp* can be blocked following exogenous addition of hCGRP.

A: Timelapse from the movies of *TrpA1*^{1} L3 Larvae fed 1h with a mixture of yeast and *Ecc* then transferred on a glass slide, in a wet chamber, to be imaged overnight. Refers to Movie 4.
B: Timelapse from the movies of *Dh31*^{KG09001}L3 Larvae fed 1h with a mixture of yeast and *Ecc* then transferred on a glass slide, in a wet chamber, to be imaged overnight. Refers to Movie 5.
C: Timelapse from the movies of w^{-} L3 Larvae fed 1h with a mixture of yeast and *Lp* + hCGRP then transferred on a glass slide, in a wet chamber, to be imaged overnight. Refers to Movie 6.
For A-C, the frames are separated by 5 minutes.

SUPP4

RNAi interference of *Dh31* in a specific subset of enteroendocrinal cells impairs the blockage phenotype.

Blockage ratio for animals expressing RNA interference constructions directed against *Dh31* mRNA, in a subset of enteroendocrine cells (DJ752-Gal4) and then fed 1h with a mixture combining yeast and *Ecc* or *Bt*. Shown is the average blockage ratio with a 95% confidence interval from at least 3 independent assays with at least 30 animals per condition and trial. ns indicates values with differences not statistically significant, **** indicates p<0,0001, Fisher exact t-test. See the source data file for details.

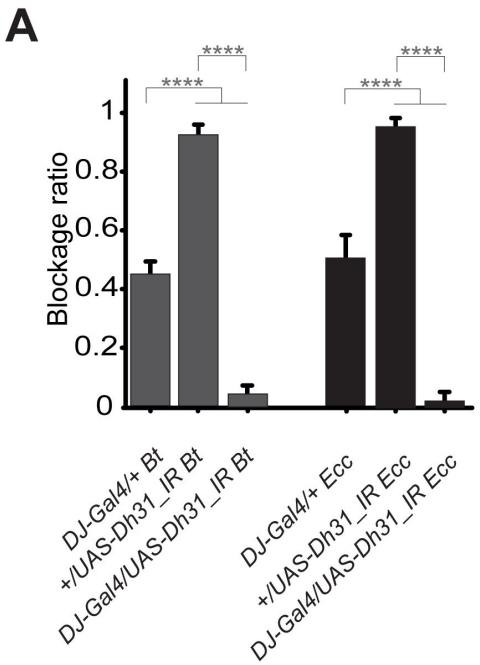

SUPP5

Uracil supplementation does not trigger the blockage phenotype.

Blockage ratio for control L3 larvae fed 1h with a mixture combining yeast and *Lp* with or without Uracil supplementation at 20 nM. Shown is the average with 95% confidence interval of at least 3 independent experiments with at least 20 larvae per trial and condition. The 0 symbol indicates an absence of blockage. ns indicates values with differences not statistically significant, Fisher exact t-test. See the source data file for details.

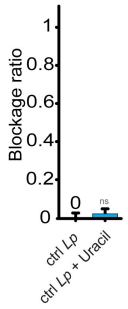

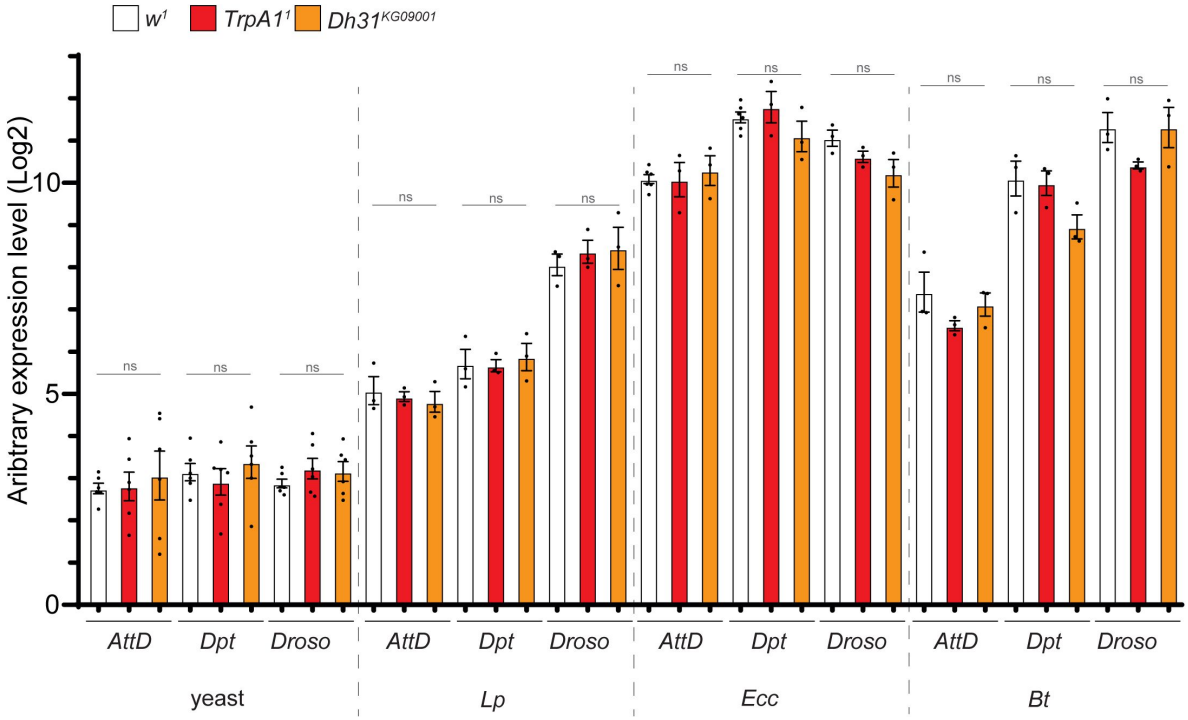

SUPP6

The intestinal immune response of reference animals, *TrpA1*^{1} and *Dh31*^{KG09001} mutants are similar.

RT-qPCR analysis of the expression of IMD/NF-kB target AMP genes Diptericin, Attacin D (AttD) and Toll target genes Drosomycin (Droso) upon enteric intoxication in w^{1} animals (reference), *TrpA1*^{1} and *Dh31*^{KG09001} mutant backgrounds. For clarity of the graph, all the statistics are not presented, but data from a full comparison between the different conditions are in the source data file (Mann Whitney test). ns Indicates p>0,05, Mann Whitney, two-tailed test. See the source data file for details. The analysis of the activation of the AMP genes was performed 5h after feeding with yeast only (yeast), yeast + *Lp* (*Lp*), yeast + *Ecc* (*Ecc*) or yeast + *Bt* (*Bt*).

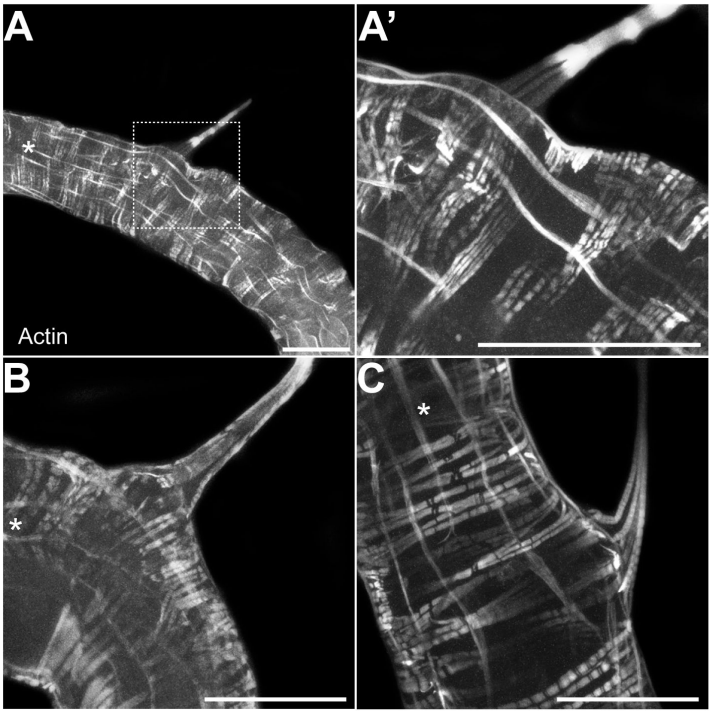

SUPP7

TARMsT2 are attached to the longitudinal gut muscles.

Confocal fluorescent pictures of different TARMsT2 in the anterior portions of L3 larval intestines to detect longitudinal and transversal muscles concentrated in actin. The white star indicates the anterior part of the intestinal portion shown. The empty square with dashed lines in A corresponds to the portion of the image magnified in A'. Scale bar represents 500µm.

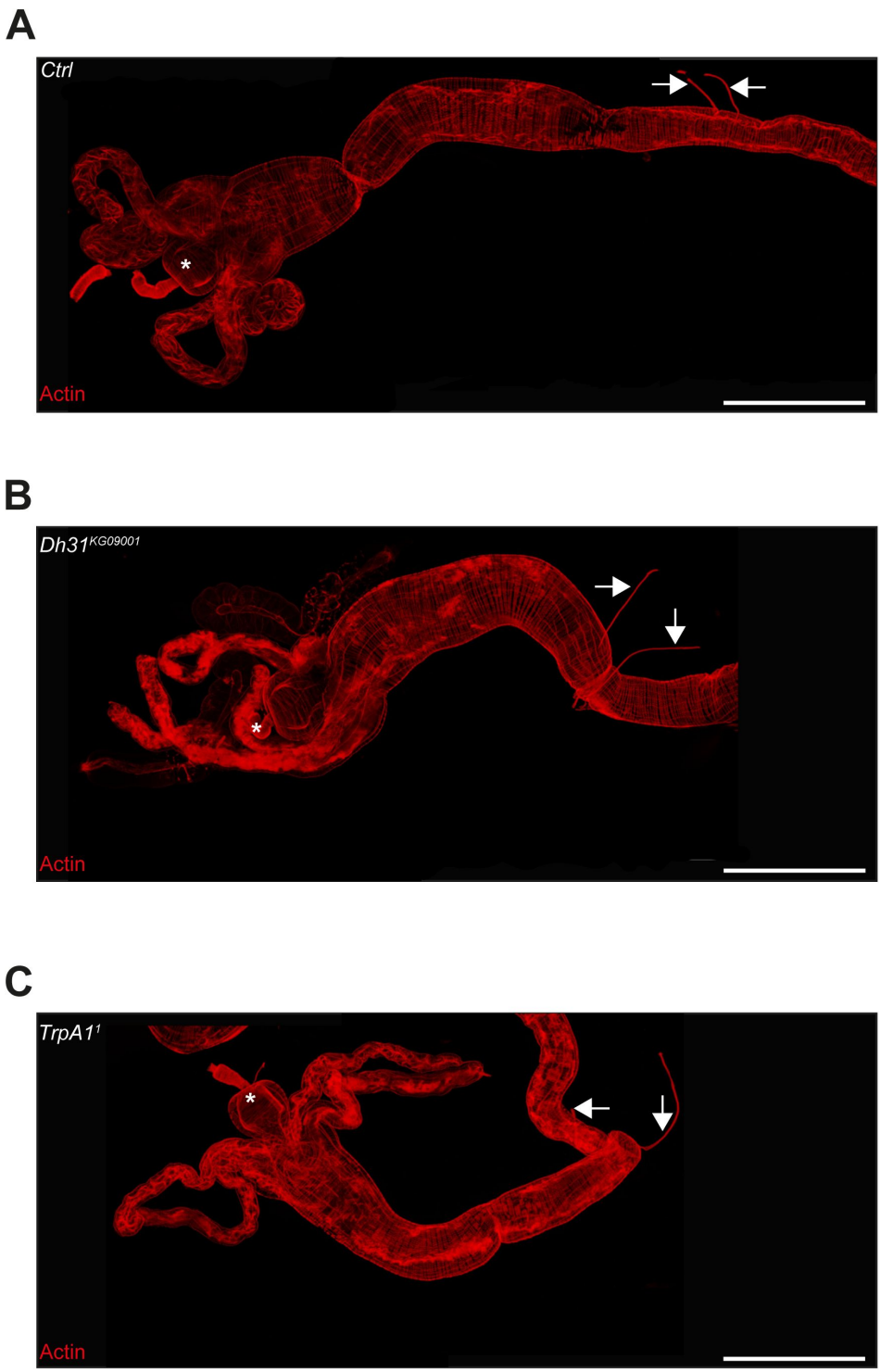

SUPP8

TARMs T2 structures are still present in *TrpA1*^{1} and *Dh31*^{KG09001} mutant backgrounds.

A: Picture to illustrate the position of the TARMs T2 structures in L3 stage CantonS larval intestine (Ctrl). The white asterisk indicates the anterior part of the intestine. Scale bar represents 500µm.
B: Picture to illustrate the position of the TARMs T2 structures in L3 stage *Dh31*^{KG09001} mutant larval intestine. The white asterisk indicates the anterior part of the intestine. Scale bar represents 500µm.
A: Picture to illustrate the position of the TARMs T2 structures in L3 stage *TrpA1*^{1} mutant larval intestine. The white asterisk indicates the anterior part of the intestine. Scale bar represents 500µm.

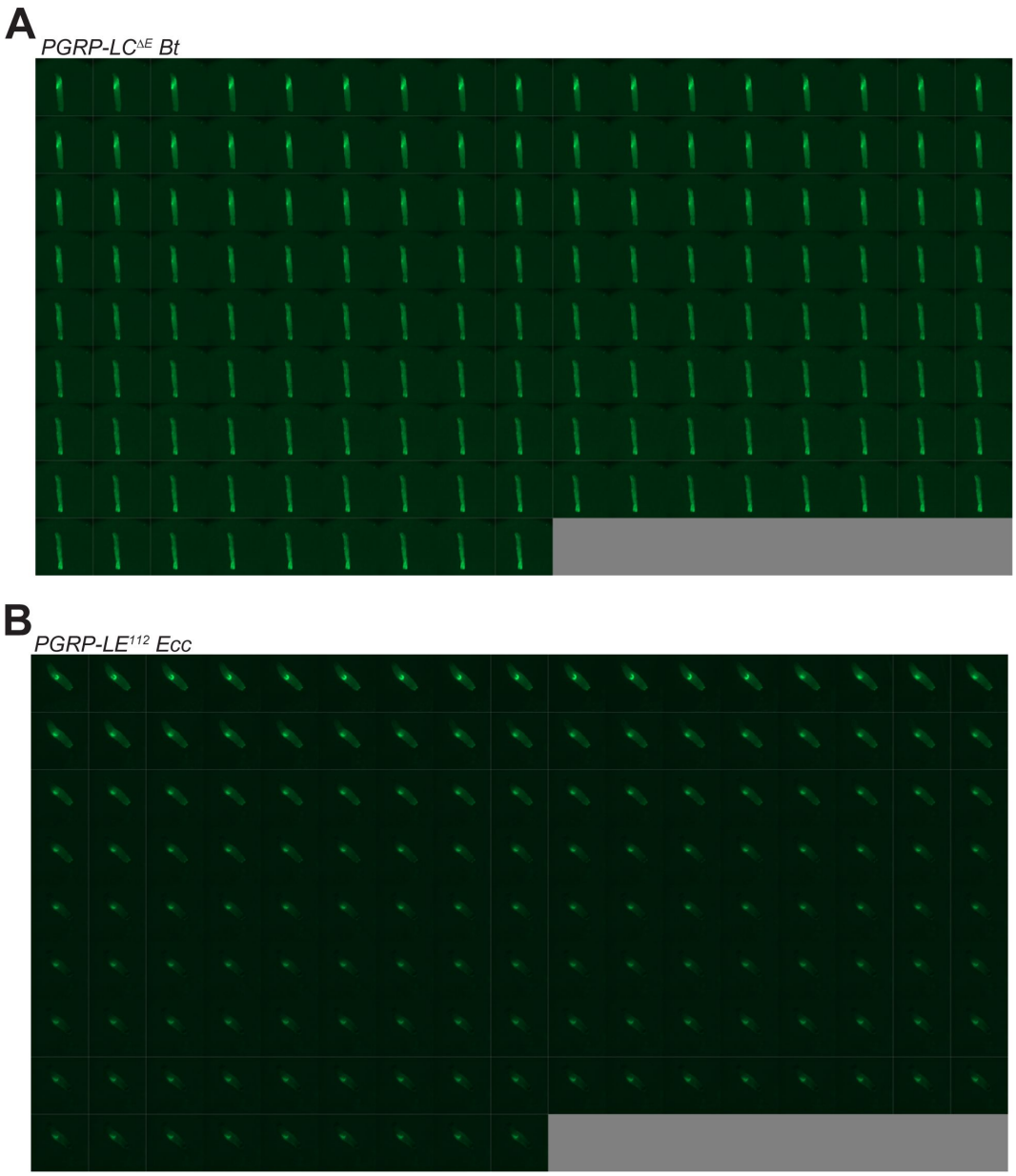

SUPP9

_Bt_ and _Ecc_ are blocked anteriorly and persist in _PGRP-LC$^{\Delta E}$ and PGRP-LE^{112}_ mutants, respectively.

A: Timelapse from the movies of _PGRP-LC$^{\Delta E}$_ L3 Larvae fed 1h with a mixture of yeast and _Bt_ then transferred on a glass slide, in a wet chamber, to be imaged overnight. Refers to Movie 8.
B: Timelapse from the movies of _PGRP-LE^{112}_ L3 Larvae fed 1h with a mixture of yeast and _Ecc_ then transferred on a glass slide, in a wet chamber, to be imaged overnight. Refers to Movie 9.
For A and B, the frames are separated by 5 minutes.

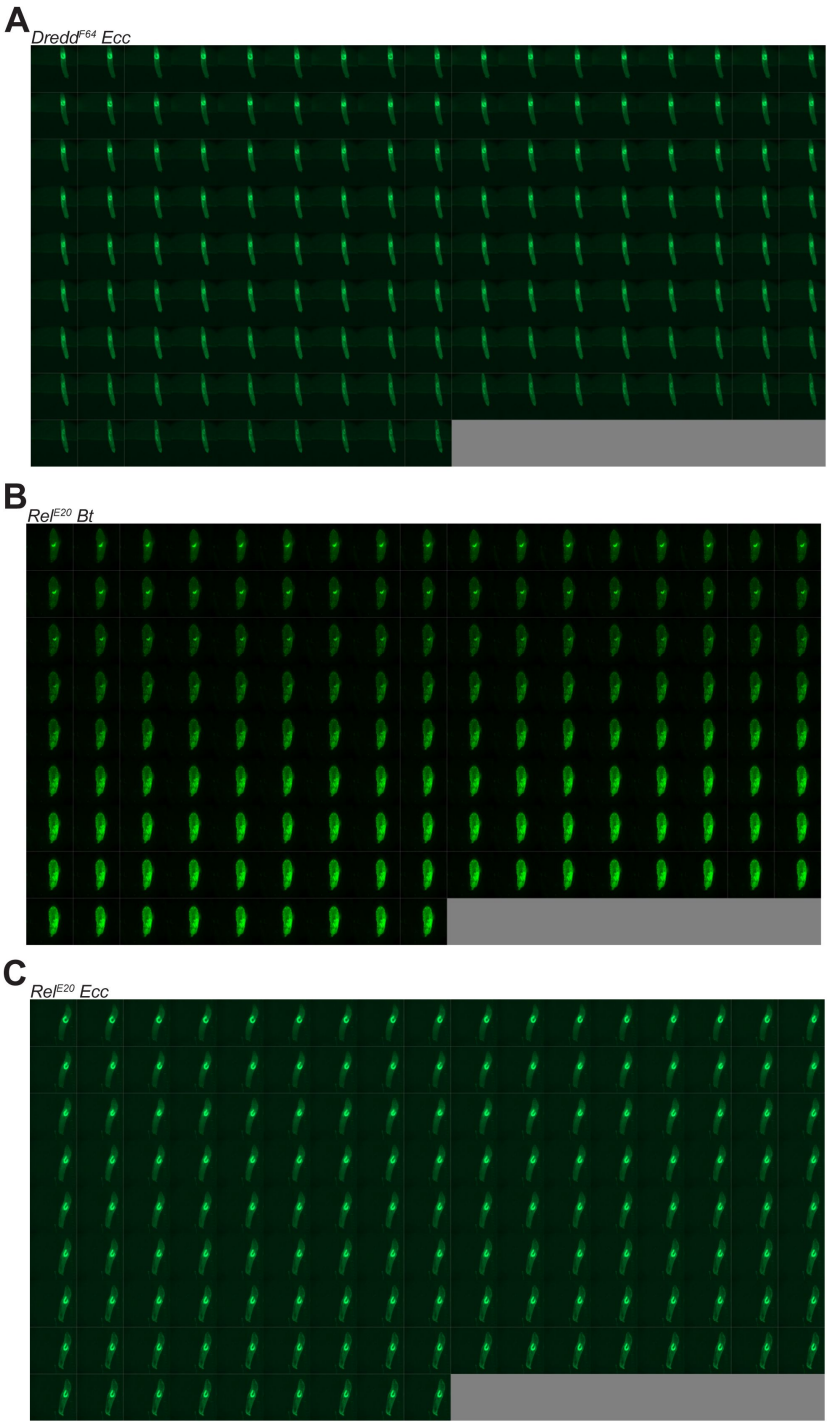

SUPP10

Bt and *Ecc* are blocked and persist anteriorly in *Dredd*^{F64} *and Rel*^{E20} mutants.

A: Timelapse from the movies of *Dredd*^{F64} L3 Larvae fed 1h with a mixture of yeast and *Ecc* then transferred on a glass slide, in a wet chamber, to be imaged overnight. Refers to Movie 10.
B: Timelapse from the movies of *Rel*^{E20} L3 Larvae fed 1h with a mixture of yeast and *Bt* then transferred on a glass slide, in a wet chamber, to be imaged overnight. Refers to Movie 11.
C: Timelapse from the movies of *Rel*^{E20} L3 Larvae fed 1h with a mixture of yeast and *Ecc* then transferred on a glass slide, in a wet chamber, to be imaged overnight. Refers to Movie 12.
For A-C, the frames are separated by 5 minutes.

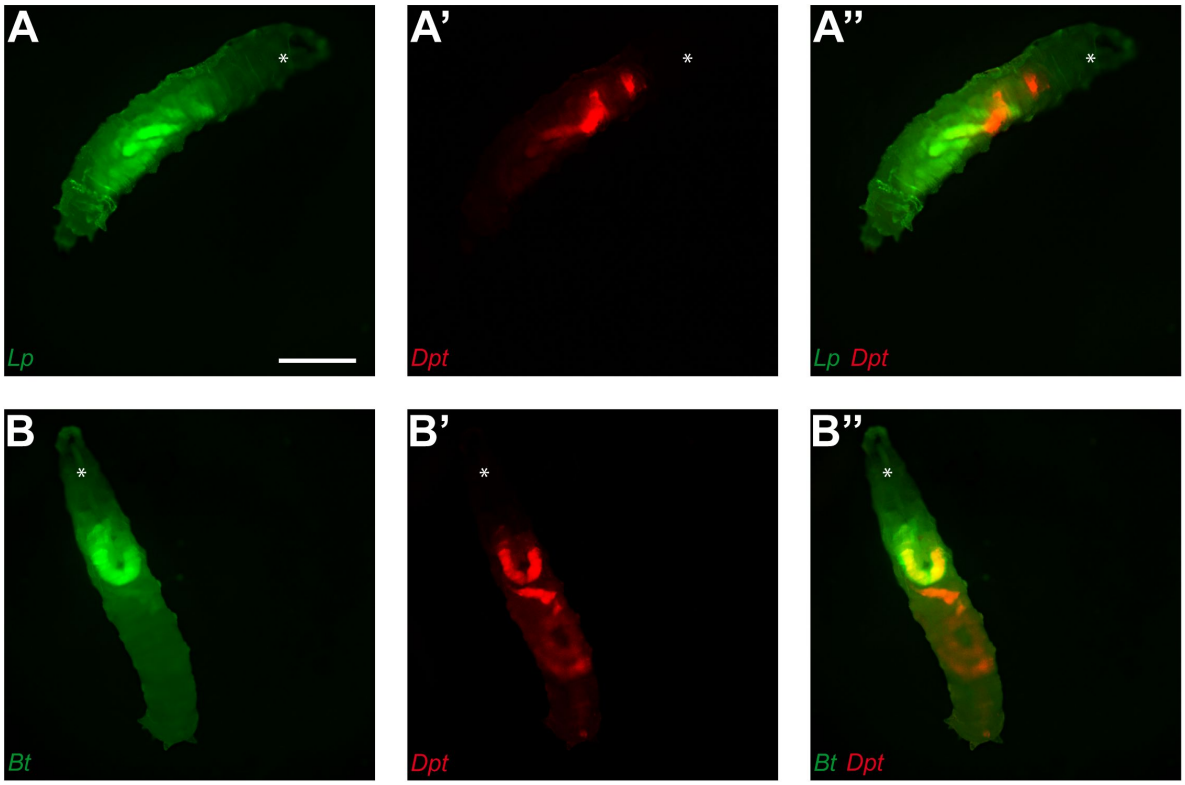

SUPP11

Fluorescent pictures of individual L3 transgenic reporter line larvae with cells expressing the *Diptericin* gene producing mCherry (A', A'', B' and B''). Larvae were fed 1h with yeast containing *Lp* (A, A' and A'') or *Bt* (B, B' and B'') then transferred on doubled sided tape in a wet chamber to be imaged 3h later. Scale bar is 1mm.

Fluorescent *Bt* is blocked in the anterior part of the larval intestine then vanishes.

Live imaging during 12h of a L3 control larva previously fed 1h with a food containing

Bt fluorescent bacteria then transferred on a glass slide in a wet chamber.

Movie 3

https://doi.org/10.6084/m9.figshare.26355076.v1

DOI: 10.6084/m9.figshare.26355076

Dextran-TexasRed is concomitantly blocked Fluorescent *Bt* in the anterior part of the larval intestine then released posteriorly following bacterial clearance.

Live imaging during 6h of a L3 control larva previously fed 1h with a food containing *Bt* fluorescent bacteria and Dextran-Texas-Red then transferred on a glass slide in a wet chamber. The anterior part of the larvae is at the bottom right.

Movie 4

https://doi.org/10.6084/m9.figshare.25018442.v2

DOI: 10.6084/m9.figshare.25018442

Fluorescent *Lp* is not blocked in the anterior part of the larval intestine and persists in the posterior midgut.

Live imaging during 10h of a L3 control larva previously fed 1h with a food containing

Lp fluorescent bacteria then transferred on a glass slide in a wet chamber.

Movie 5

https://doi.org/10.6084/m9.figshare.26355196.v1

DOI: 10.6084/m9.figshare.26355196

***Bt* at a low concentration is not blocked in the anterior part of the larval intestine, persists in the posterior midgut and the larva does not die.**

Live imaging during 10h of a L3 control larva previously fed 1h with a food containing *Bt* fluorescent bacteria (1.10^{10} bacteria per ml instead of 4.10^{10}) then transferred on a glass slide in a wet chamber.

Movie 6

https://doi.org/10.6084/m9.figshare.25018463.v1

DOI: 10.6084/m9.figshare.25018463

Fluorescent *Ecc* is not blocked in the anterior part of the *TrpA1* mutant larval intestine and persists in the posterior midgut.

Live imaging during 10h of a L3 *TrpA1* mutant larva previously fed 1h with a food containing *Ecc* fluorescent bacteria then transferred on a glass slide in a wet chamber.

Movie 7

https://doi.org/10.6084/m9.figshare.25018472.v1

DOI: 10.6084/m9.figshare.25018472

Fluorescent *Ecc* is not blocked in the anterior part of the *Dh31* mutant larval intestine and persists in the posterior midgut.

Live imaging during 10h of a L3 *Dh31* mutant larva previously fed 1h with a food containing *Ecc* fluorescent bacteria then transferred on a glass slide in a wet chamber.

Movie 8

https://doi.org/10.6084/m9.figshare.25018481.v1

DOI: 10.6084/m9.figshare.25018481

Fluorescent *Lp* is blocked in the anterior part of the larval intestine following treatment with hCGRP.

Live imaging during 12h of a control L3 larva previously fed 1h with a food containing

Lp fluorescent bacteria and hCGRP then transferred on a glass slide in a wet chamber.

Movie 9

https://doi.org/10.6084/m9.figshare.27100474.v1

DOI: 10.6084/m9.figshare.27100474

Robust muscular contraction waves are observed in intestines of *Dh31* mutant larvae previously fed with *Ecc*.

Live imaging of a L3 *Dh31* mutant larval intestine. The animal was previously fed 1h with a food containing *Ecc* fluorescent bacteria and the dissected gut was then transferred in Schneider media.

Movie 10

https://doi.org/10.6084/m9.figshare.27100483.v1

DOI: 10.6084/m9.figshare.27100483

Robust muscular contraction waves are observed in intestines of *Dh31* mutant larvae.

Live imaging of a L3 *Dh31* mutant larval intestine. The animal was previously fed 1h with a food mixture that did not contain bacteria and the dissected gut was then transferred in Schneider media.

Movie 11

https://doi.org/10.6084/m9.figshare.25018496.v1

DOI: 10.6084/m9.figshare.25018496

TARMsT2 are attached to the longitudinal gut muscles.

Confocal imaging of the intestine from a control animal stained with fluorescent phalloidin and animated 3D-reconstruction of the anterior portion containing the attached TARMs.

Movie 12

https://doi.org/10.6084/m9.figshare.25018499.v1

DOI: 10.6084/m9.figshare.25018499

Fluorescent *Bt* is blocked in the anterior part of the *PGRP-LC* mutant larval intestine and persists.

Live imaging during 12h of a L3 *PGRP-LC* mutant larva previously fed 1h with a food containing *Bt* fluorescent bacteria then transferred on a glass slide in a wet chamber.

Movie 13

https://doi.org/10.6084/m9.figshare.25018505.v1

DOI: 10.6084/m9.figshare.25018505

Fluorescent *Ecc* is blocked in the anterior part of the *PGRP-LE* mutant larval intestine and persists.

Live imaging during 12h of a L3 *PGRP-LE* mutant larva previously fed 1h with a food containing *Ecc* fluorescent bacteria then transferred on a glass slide in a wet chamber.

Movie 14

https://doi.org/10.6084/m9.figshare.25018517.v1

DOI: 10.6084/m9.figshare.25018517

Fluorescent *Ecc* is blocked in the anterior part of the *Dredd* mutant larval intestine and persists.

Live imaging during 12h of a L3 *Dredd* mutant larva previously fed 1h with a food containing *Ecc* fluorescent bacteria then transferred on a glass slide in a wet chamber.

Movie 15

https://doi.org/10.6084/m9.figshare.25018529.v1

DOI: 10.6084/m9.figshare.25018529

Fluorescent *Bt* is blocked in the anterior part of the *Rel* mutant larval intestine and persists.

Live imaging during 12h of a L3 *Rel* mutant larva previously fed 1h with a food containing *Bt* fluorescent bacteria then transferred on a glass slide in a wet chamber.

Movie 16

https://doi.org/10.6084/m9.figshare.25018538.v1

DOI: 10.6084/m9.figshare.25018538

Fluorescent *Ecc* is blocked in the anterior part of the *Rel* mutant larval intestine and persists.

Live imaging during 12h of a L3 *Rel* mutant larva previously fed 1h with a food containing *Ecc* fluorescent bacteria then transferred on a glass slide in a wet chamber.

Author contributions

L.K., A.G., F.T., M.M., O.P., D.O. and J.R. conceived the experiments. F.T., M.M., O.P. and R.M. performed the experiments. L.K., A.G., F.T., D.O. and J.R. wrote the manuscript. A.G., D.O. and J.R. secured funding.

Competing interests

The authors have declared that no competing interests exist.

Acknowledgements

We are grateful to all members of the BES and DEB teams at the Institut Sophia Agrobiotech for fruitful discussions. We greatly thank Emilie Avazéri, Ambre Bigot, Elisa Di Lelio, Juliette Dubois, Marie-Paule Esposito and Gladys Gazelle for their technical support. We thank Bernard Charroux (at the IBDM Aix Marseille University) and Ambra MASUZZO (in the team of Richard Benton, Université de Lausanne) for pioneer observations and numerous discussions, François Leulier and Renata Matos for sharing bacterial and fly lines and Frank Schnorrer for discussions about alary muscles.

Funding

F.T. was supported by the Lebanese Association for Scientific Research (LASER), the AJAJE association from Lebanon, and the Université Côte d'Azur (ATER). This work was supported by the French government through the UCAJEDI Investments in the Future project managed by the

National Research Agency (ANR) with the reference number ANR-15-IDEX-01 and through the ANR-22-CE35-0006-01 (BaDAss) to A.G. This work was supported by CNRS, ANR BACNEURODRO (ANR-17-CE16-0023-01),

Equipe Fondation pour la Recherche Médicale (EQU201603007783) and the ANR Pepneuron (ANR-21-CE16-0027) to J.R. and L.K.

References

Arias-Rojas A., Frahm D., Hurwitz R., Brinkmann V., Iatsenko I (2023) **Resistance to host antimicrobial peptides mediates resilience of gut commensals during infection and aging in Drosophila** *Proc Natl Acad Sci U S A* **120**

Basset A., Khush R. S., Braun A., Gardan L., Boccard F., Hoffmann J. A., Lemaitre B (2000) **The phytopathogenic bacteria Erwinia carotovora infects Drosophila and activates an immune response** *Proc Natl Acad Sci U S A* **97**:3376–81

Bataillé L., Colombié N., Pelletier A., Paululat A., Lebreton G., Carrier Y., Frendo J. L., Vincent A (2020) **Alary muscles and thoracic alary-related muscles are atypical striated muscles involved in maintaining the position of internal organs** *Development* **147**

Belinskaia M., Wang J., Kaza S. K., Antoniazzi C., Zurawski T., Dolly J. O., Lawrence G. W. (2023) **Bipartite Activation of Sensory Neurons by a TRPA1 Agonist Allyl Isothiocyanate Is Reflected by Complex Ca(2+) Influx and CGRP Release Patterns: Enhancement by NGF and Inhibition with VAMP and SNAP-25 Cleaving Botulinum Neurotoxins** *Int J Mol Sci* **24**

Benguettat O., Jneid R., Soltys J., Loudhaief R., Brun-Barale A., Osman D., Gallet A (2018) **The DH31/CGRP enteroendocrine peptide triggers intestinal contractions favoring the elimination of opportunistic bacteria** *PLoS Pathog* **14** https://doi.org/10.1371/journal.ppat.1007279

Bosco-Drayon V., Poidevin M., Boneca I. G., Narbonne-Reveau K., Royet J., Charroux B (2012) **Peptidoglycan sensing by the receptor PGRP-LE in the Drosophila gut induces immune responses to infectious bacteria and tolerance to microbiota** *Cell Host Microbe* **12**:153–65

Bulc M., Palus K., Całka J., Zielonka Ł (2018) **Changes in Immunoreactivity of Sensory Substances within the Enteric Nervous System of the Porcine Stomach during Experimentally Induced Diabetes** *J Diabetes Res* **2018**

Capo F., Wilson A., Di Cara F. (2019) **The Intestine of Drosophila melanogaster: An Emerging Versatile Model System to Study Intestinal Epithelial Homeostasis and Host-Microbial Interactions in Humans** *Microorganisms* **7** https://doi.org/10.3390/microorganisms7090336

Carboni A. L., Hanson M. A., Lindsay S. A., Wasserman S. A., Lemaitre B (2022) **Cecropins contribute to Drosophila host defense against a subset of fungal and Gram-negative bacterial infection** *Genetics* **220**

Chakrabarti S., Liehl P., Buchon N., Lemaitre B (2012) **Infection-induced host translational blockage inhibits immune responses and epithelial renewal in the Drosophila gut** *Cell Host Microbe* **12**:60–70 https://doi.org/10.1016/j.chom.2012.06.001

Chen J., Kim S. M., Kwon J. Y. (2016) **A Systematic Analysis of Drosophila Regulatory Peptide Expression in Enteroendocrine Cells** *Molecules and Cells* https://doi.org/10.14348/molcells.2016.0014

Dombrovski M., Kim A., Poussard L., Vaccari A., Acton S., Spillman E., Condron B., Yuan Q (2019) **A Plastic Visual Pathway Regulates Cooperative Behavior in Drosophila Larvae** *Curr Biol* **29**:1866–1876

Dombrovski M., Poussard L., Moalem K., Kmecova L., Hogan N., Schott E., Vaccari A., Acton S., Condron B (2017) **Cooperative Behavior Emerges among Drosophila Larvae** *Curr Biol* **27**:2821–2826

Du E. J. *et al.* (2016) **TrpA1 Regulates Defecation of Food-Borne Pathogens under the Control of the Duox Pathway** *PLoS Genet* **12** https://doi.org/10.1371/journal.pgen.1005773

Du E. J., Ahn T. J., Wen X., Seo D. W., Na D. L., Kwon J. Y., Choi M., Kim H. W., Cho H., Kang K (2016) **Nucleophile sensitivity of Drosophila TRPA1 underlies light-induced feeding deterrence** *Elife* **5**

Earl S. C., Rogers M. T., Keen J., Bland D. M., Houppert A. S., Miller C., Temple I., Anderson D. M., Marketon M. M (2015) **Resistance to Innate Immunity Contributes to Colonization of the Insect Gut by Yersinia pestis** *PLoS One* **10**

Gu P., Gong J., Shang Y., Wang F., Ruppell K. T., Ma Z., Sheehan A. E., Freeman M. R., Xiang Y (2019) **Polymodal Nociception in Drosophila Requires Alternative Splicing of TrpA1** *Curr Biol* **29**:3961–3973

Guntur A. R., Gu P., Takle K., Chen J., Xiang Y., Yang C. H (2015) **Drosophila TRPA1 isoforms detect UV light via photochemical production of H2O2** *Proc Natl Acad Sci U S A* **112**:E5753–61

Guo X., Lv J., Xi R (2021) **The specification and function of enteroendocrine cells in Drosophila and mammals: a comparative review** *Febs j*

Ha E. M., Lee K. A., Seo Y. Y., Kim S. H., Lim J. H., Oh B. H., Kim J., Lee W. J (2009) **Coordination of multiple dual oxidase-regulatory pathways in responses to commensal and infectious microbes in drosophila gut** *Nat Immunol* **10**:949–57 https://doi.org/10.1038/ni.1765

Ha E. M., Oh C. T., Bae Y. S., Lee W. J (2005) **A direct role for dual oxidase in Drosophila gut immunity** *Science* **310**:847–50

Hachfi S. *et al.* (2024) **Ingestion of Bacillus cereus spores dampens the immune response to favor bacterial persistence** *Nat Commun* **15**

Hanson M. A., Lemaitre B (2020) **New insights on Drosophila antimicrobial peptide function in host defense and beyond** *Curr Opin Immunol* **62**:22–30

Hegedus D., Erlandson M., Gillott C., Toprak U (2009) **New insights into peritrophic matrix synthesis, architecture, and function** *Annu Rev Entomol* **54**:285–302

Kaneko T. *et al.* (2006) **PGRP-LC and PGRP-LE have essential yet distinct functions in the drosophila immune response to monomeric DAP-type peptidoglycan** *Nat Immunol* **7**:715–23

Kasacka I (2009) **Quantitative distribution and localization of calcitonin gene-related peptide-like cells in the stomach of two kidney, one clip rats** *J Physiol Pharmacol* **60**:35–9

Keita S., Masuzzo A., Royet J., Kurz C. L. (2017) **Drosophila larvae food intake cessation following exposure to Erwinia contaminated media requires odor perception, Trpa1 channel and evf virulence factor** *J Insect Physiol* **99**:25–32 https://doi.org/10.1016/j.jinsphys.2017.02.004

Kim E. K., Lee K. A., Hyeon D. Y., Kyung M., Jun K. Y., Seo S. H., Hwang D., Kwon Y., Lee W. J (2020) **Bacterial Nucleoside Catabolism Controls Quorum Sensing and Commensal-to-Pathogen Transition in the Drosophila Gut** *Cell Host Microbe* **27**:345–357

Kondo T., Oshima T., Obata K., Sakurai J., Knowles C. H., Matsumoto T., Noguchi K., Miwa H (2010) **Role of transient receptor potential A1 in gastric nociception** *Digestion* **82**:150–5

Kunst M., Hughes M. E., Raccuglia D., Felix M., Li M., Barnett G., Duah J., Nitabach M. N (2014) **Calcitonin gene-related peptide neurons mediate sleep-specific circadian output in Drosophila** *Curr Biol* **24**:2652–64

LaJeunesse D. R., Johnson B., Presnell J. S., Catignas K. K., Zapotoczny G (2010) **Peristalsis in the junction region of the Drosophila larval midgut is modulated by DH31 expressing enteroendocrine cells** *BMC Physiol* **10** https://doi.org/10.1186/1472-6793-10-14

Lanan M. C., Rodrigues P. A., Agellon A., Jansma P., Wheeler D. E (2016) **A bacterial filter protects and structures the gut microbiome of an insect** *Isme j* **10**:1866–76

Lapointe T. K., Altier C. (2011) **The role of TRPA1 in visceral inflammation and pain** *Channels* **5**:525–529 https://doi.org/10.4161/chan.5.6.18016

Lee K. A., Kim S. H., Kim E. K., Ha E. M., You H., Kim B., Kim M. J., Kwon Y., Ryu J. H., Lee W. J (2013) **Bacterial-derived uracil as a modulator of mucosal immunity and gut-microbe homeostasis in Drosophila** *Cell* **153**:797–811 https://doi.org/10.1016/j.cell.2013.04.009

Lemaitre B., Miguel-Aliaga I (2013) **The digestive tract of Drosophila melanogaster** *Annu Rev Genet* **47**:377–404 https://doi.org/10.1146/annurev-genet-111212-133343

Leulier F., Parquet C., Pili-Floury S., Ryu J. H., Caroff M., Lee W. J., Mengin-Lecreulx D., Lemaitre B (2003) **The Drosophila immune system detects bacteria through specific peptidoglycan recognition** *Nat Immunol* **4**:478–84

Louis M., de Polavieja G. (2017) **Collective Behavior: Social Digging in Drosophila Larvae** *Curr Biol* **27**:R1010–r1012

Mast J. D., De Moraes C. M., Alborn H. T., Lavis L. D., Stern D. L. (2014) **Evolved differences in larval social behavior mediated by novel pheromones** *Elife* **3**

Nardi J. B., Bee C. M., Taylor S. J (2016) **Compartmentalization of microbial communities that inhabit the hindguts of millipedes** *Arthropod Struct Dev* **45**:462–474

Nässel D. R., Zandawala M (2019) **Recent advances in neuropeptide signaling in Drosophila, from genes to physiology and behavior** *Prog Neurobiol* **179**

Nawrot-Esposito M. P., Babin A., Pasco M., Poirié M., Gatti J. L., Gallet A (2020) **Bacillus thuringiensis Bioinsecticides Induce Developmental Defects in Non-Target Drosophila melanogaster Larvae** *Insects* **11**

Neyen C., Bretscher A. J., Binggeli O., Lemaitre B (2014) **Methods to study Drosophila immunity** *Methods* **68**:116–28 https://doi.org/10.1016/j.ymeth.2014.02.023

Ogawa N., Kurokawa T., Mori Y (2016) **Sensing of redox status by TRP channels** *Cell Calcium* **60**:115–22 https://doi.org/10.1016/j.ceca.2016.02.009

Park D., Veenstra J. A., Park J. H., Taghert P. H (2008) **Mapping peptidergic cells in Drosophila: where DIMM fits in** *PLoS One* **3** https://doi.org/10.1371/journal.pone.0001896

Pelaseyed T. *et al.* (2014) **The mucus and mucins of the goblet cells and enterocytes provide the first defense line of the gastrointestinal tract and interact with the immune system** *Immunol Rev* **260**:8–20 https://doi.org/10.1111/imr.12182

Ramond E., Jamet A., Ding X., Euphrasie D., Bouvier C., Lallemant L., He X., Arbibe L., Coureuil M., Charbit A (2021) **Reactive Oxygen Species-Dependent Innate Immune Mechanisms Control Methicillin-Resistant Staphylococcus aureus Virulence in the Drosophila Larval Model** *MBio* **12**

Ryu J. H., Ha E. M., Oh C. T., Seol J. H., Brey P. T., Jin I., Lee D. G., Kim J., Lee D., Lee W. J (2006) **An essential complementary role of NF-kappaB pathway to microbicidal oxidants in Drosophila gut immunity** *EMBO J* **25**:3693–701

Ryu J. H., Kim S. H., Lee H. Y., Bai J. Y., Nam Y. D., Bae J. W., Lee D. G., Shin S. C., Ha E. M., Lee W. J (2008) **Innate immune homeostasis by the homeobox gene caudal and commensal-gut mutualism in Drosophila** *Science* **319**:777–82 https://doi.org/10.1126/science.1149357

Stenbak C. R. *et al.* (2004) **Peptidoglycan molecular requirements allowing detection by the Drosophila immune deficiency pathway** *J Immunol* **173**:7339–48

Storelli G., Strigini M., Grenier T., Bozonnet L., Schwarzer M., Daniel C., Matos R., Leulier F (2018) **Drosophila Perpetuates Nutritional Mutualism by Promoting the Fitness of Its Intestinal Symbiont Lactobacillus plantarum** *Cell Metab* **27**:362–377 https://doi.org/10.1016/j.cmet.2017.11.011

Surendran S., Huckesfeld S., Waschle B., Pankratz M. J (2017) **Pathogen-induced food evasion behavior in Drosophila larvae** *J Exp Biol* **220**:1774–1780 https://doi.org/10.1242/jeb.153395

Veenstra J. A., Agricola H. J., Sellami A (2008) **Regulatory peptides in fruit fly midgut** *Cell Tissue Res* **334**:499–516 https://doi.org/10.1007/s00441-008-0708-3

Vodovar N., Vinals M., Liehl P., Basset A., Degrouard J., Spellman P., Boccard F., Lemaitre B (2005) **Drosophila host defense after oral infection by an entomopathogenic Pseudomonas species** *Proc Natl Acad Sci U S A* **102**:11414–9

Yao Z., Cai Z., Ma Q., Bai S., Wang Y., Zhang P., Guo Q., Gu J., Lemaitre B., Zhang H (2022) **Compartmentalized PGRP expression along the dipteran Bactrocera dorsalis gut forms a zone of protection for symbiotic bacteria** *Cell Rep* **41**

Younes S., Al-Sulaiti A., Nasser E. A. A., Najjar H., Kamareddine L (2020) **Drosophila as a Model Organism in Host-Pathogen Interaction Studies** *Front Cell Infect Microbiol* **10**

Zaidman-Rémy A., Regan J. C., Brandão A. S., Jacinto A (2012) **The Drosophila larva as a tool to study gut-associated macrophages: PI3K regulates a discrete hemocyte population at the proventriculus** *Dev Comp Immunol* **36**:638–47

Zhai Z., Huang X., Yin Y (2018) **Beyond immunity: The Imd pathway as a coordinator of host defense, organismal physiology and behavior** *Dev Comp Immunol* **83**:51–59

Editors

Reviewing Editor
Bruno Lemaitre
École Polytechnique Fédérale de Lausanne, Lausanne, Switzerland

Senior Editor
Utpal Banerjee
University of California, Los Angeles, Los Angeles, United States of America

Reviewer #1 (Public review):

Tleiss et al. demonstrate that while commensal Lactiplantibacillus plantarum freely circulate within the intestinal lumen, pathogenic strains such as Erwinia carotovora or Bacillus thuringiensis are blocked in the anterior midgut where they are rapidly eliminated by antimicrobial peptides. This sequestration of pathogenic bacteria in the anterior midgut requires the Duox enzyme in enterocytes, and both TrpA1 and Dh31 in enteroendocrine cells. This effect induces muscular muscle contraction, which is marked by the formation of TARM structures (thoracic ary-related muscles). This muscle contraction-related blocking happens early after infection (15mins). On the other side, the clearance of bacteria is done by the IMD pathway possibly through antimicrobial peptide production while it is dispensable for the blockage. Genetic manipulations impairing bacterial compartmentalization result in abnormal colonization of posterior midgut regions by pathogenic bacteria. Despite a functional IMD pathway, this ectopic colonization leads to bacterial proliferation and larval death, demonstrating the critical role of bacteria anterior sequestration in larval defense.

In general, this fundamentally important study reveals unique mechanisms in the gut immunity of Drosophila larvae. It also describes a previously understudied structure, TARM, which may play a crucial role in this process. This significant work substantially advances our understanding of pathogen clearance by identifying a new mode of pathogen eradication from the insect gut. The evidence supporting the authors' claims is compelling, and the study opens new avenues for future research in gut immunity.

https://doi.org/10.7554/eLife.98716.2.sa2

Reviewer #2 (Public review):

Summary:

This article describes a novel mechanism of host defense in the gut of Drosophila larvae. Pathogenic bacteria trigger the activation of a valve that blocks them in the anterior midgut where they are subjected to the action of antimicrobial peptides. In contrast, beneficial symbiotic bacteria do not activate the contraction of this sphincter and can access the posterior midgut, a compartment more favorable to bacterial growth.

Strengths:

The authors decipher the underlying mechanism of sphincter contraction, revealing that ROS production by Duox activates the release of DH31 by enteroendocrine cells that stimulate visceral muscle contractions. Use of mutations affecting the Imd pathway or lacking

antimicrobial peptides reveals their contribution to pathogen elimination in the anterior midgut.

Weaknesses:

The mechanism allowing the discrimination between commensal and pathogenic bacteria remains unclear.

https://doi.org/10.7554/eLife.98716.2.sa1

Author response:

The following is the authors' response to the original reviews.

> ***Reviewer #1 (Public Review):***
>
> *Tleiss et al. demonstrate that while commensal Lactiplantibacillus plantarum freely circulate within the intestinal lumen, pathogenic strains such as Erwinia carotovora or Bacillus thuringiensis are blocked in the anterior midgut where they are rapidly eliminated by antimicrobial peptides. This sequestration of pathogenic bacteria in the anterior midgut requires the Duox enzyme in enterocytes, and both TrpA1 and Dh31 in enteroendocrine cells. This effect induces muscular muscle contraction, which is marked by the formation of TARM structures (thoracic ary-related muscles). This muscle contraction-related blocking happens early after infection (15mins). On the other side, the clearance of bacteria is done by the IMD pathway possibly through antimicrobial peptide production while it is dispensable for the blockage. Genetic manipulations impairing bacterial compartmentalization result in abnormal colonization of posterior midgut regions by pathogenic bacteria. Despite a functional IMD pathway, this ectopic colonization leads to bacterial proliferation and larval death, demonstrating the critical role of bacteria anterior sequestration in larval defense.*
>
> *This important work substantially advances our understanding of the process of pathogen clearance by identifying a new mode of pathogen eradication from the insect gut. The evidence supporting the authors' claims is solid and would benefit from more rigorous experiments.*
>
> *(1) The authors performed the experiments on Drosophila larvae. I wonder whether this model could extend to adult flies since they have shown that the ROS/TRPA1/Dh31 axis is important for gut muscle contraction in adult flies. If not, how would the authors explain the discrepancy between larvae and adults?*

We have linked the adult phenotype to the larval model to explore the ROS/TrpA1/Dh31 axis in both contexts. As highlighted in the discussion, however, there are key behavioral differences between larvae and adult flies. Unlike larvae, which remain in the food environment, adult flies have the ability to move away. This difference could impact the relevance of gut muscle contraction and bacterial clearance mechanisms between the two stages. Specifically, in larvae, the rapid ejection of gut contents due to muscle contraction poses a unique risk: larvae may inadvertently re-ingest the expelled material within minutes, which could influence their immune defenses. We have clarified this distinction and our hypothesis in the final section of the discussion, as it emphasizes the adaptive nature of this mechanism in larvae.

> *(2) The authors performed their experiments and proposed the models based on two pathogenic bacteria and one commensal bacterial at a relatively high bacterial dose.*

> *They showed that feeding Bt at 2X1010 or Ecc15 at 4X108 did not induce a blockage phenotype.*
>
> *I wonder whether larvae die under conditions of enteric infection with low concentrations of pathogenic bacteria.*

To address this, we have provided new data (Movie 5), in which larvae were fed a lower dose of Bt-GFP at 1.3 × 10^10 CFU/mL. In this video, we observe that when larvae ingest fewer bacteria, no blockage occurs, and the bacteria are able to reach the posterior midgut. As the bacterial load is lower, the fluorescence signal is weaker, but the movie clearly shows the excretion of bacteria. Importantly, under these conditions, no larval death was observed. These findings suggest that below a certain bacterial threshold, the pathogenicity is insufficient to: (1) trigger the blockage response, and (2) kill the larvae. In such cases, bacteria are likely eliminated through normal peristaltic movements rather than through the blockage mechanism described in our study.

> *If larvae do not show mortality, what is the mechanism for resisting low concentrations of pathogenic bacteria?*

As mentioned in our previous response, we hypothesize that the larvae's ability to resist low concentrations of pathogenic bacteria is likely due to being below the threshold of virulence. At lower bacterial doses, the pathogenic load is insufficient to trigger the blockage mechanism or cause larval death. In these cases, it is probable that classical peristaltic movements of the gut efficiently eliminate the bacteria, preventing them from colonizing the posterior midgut or causing significant harm. Thus, the larvae rely on standard gut motility and immune mechanisms, rather than the blockage response, to clear lower doses of bacteria.

> *Why is this model only applied to high-dose infections?*

The reason this model primarily applies to high-dose infections is that lower concentrations of pathogenic bacteria do not trigger the blockage mechanism. As we mentioned in the manuscript, for low bacterial concentrations, where the GFP signal remains detectable, wild-type larvae are still able to resist live bacteria in the posterior part of the intestine.

Regarding the bacterial doses used in our experiments, it's important to clarify that we calculate the bacterial load based on colony-forming units (CFU). In our setup, there are approximately 5 × 10^4 CFU per midgut. For each experiment, we prepare 500 µl of contaminated medium containing 4 × 10^10 CFU. Fifty larvae are placed into this 500 µl of medium, meaning each larva ingests around 5 × 10^4 CFU within one hour of feeding.

This leads us to two key points:

(1) Continuous feeding might trigger the blockage response even at lower doses, as extended exposure to bacteria could lead to higher accumulation within the gut.

(2) Other defense mechanisms, such as the production of reactive oxygen species (ROS) or classical peristaltic movements, could be sufficient to eliminate lower bacterial doses (around 10^3 CFU or below).

We also refer to the newly provided Movie 5, where larvae fed with Bt-GFP at 1.3 × 10^10 CFU/mL show no blockage at low ingestion levels and successfully eliminate the bacteria.

> *(3) The authors claim that the lock of bacteria happens at 15 minutes while killing by AMPs happens 6-8 hours later.*

Our CFU data indicate that it's after 4 to 6 hours that the quantity of bacteria decreases. We fixed this in the text.

> *What happened during this period?*

During the 4 to 6-hour period, several defense mechanisms are activated. ROS play a bacteriostatic and bacteriolytic role, helping to control bacterial growth. Concurrently, the IMD pathway is activated, leading to the transcription, translation, and secretion of antimicrobial peptides. These AMPs exert both bacteriostatic and bacteriolytic effects, contributing to the eventual clearance of the pathogenic bacteria.

> *More importantly, is IMD activity induced in the anterior region of the larval gut in both Ecc15 and Bt infection at 6 hours after infection?*

We have provided new data (Supplementary Figure 6) that includes RT-qPCR analysis of the whole larval gut in wt, TrpA1- and Dh31- genetic background after feeding with Lp, Ecc15, Bt, or yeast only. We monitored the expression of three different AMP-encoding genes and found that while AMP expression varied depending on the food content, there were no significant differences between the genotypes tested.

Additionally, we included new imaging data (Supplementary Figure 11) from AMP reporter larvae (*Dpt*-Cherry) fed with fluorescent Lp or Bt. In larvae infected with Bt, which is blocked in the anterior part of the gut, the *dpt* gene is predominantly induced in this region, indicating strong IMD pathway activity in response to Bt infection. Conversely, in larvae fed with Lp-GFP, the *Dpt*-Cherry reporter shows weak expression in the anterior midgut, and is barely detectable in the posterior midgut where Lp-GFP establishes itself. This aligns with previous findings by Bosco-Drayon et al. (2012), which demonstrated low AMP expression in the posterior midgut due to the presence of negative regulators of the IMD pathway, such as amidases and Pirk.

> *Are they mostly expressed in the anterior midgut in both bacterial infections? Several papers have shown quite different IMD activity patterns in the Drosophila gut. Zhai et al. have shown that in adult Drosophila, IMD activity was mostly absent in the R2 region as indicated by dpt-lacZ. Vodovar et al. have shown that the expression of dpt-lacZ is observable in proventriculus while Pe is not in the same region. Tzou et al. showed that Ecc15 infection induced IMD activity in the anterior midgut 24 hours after infection.*

Based on our new data (Supplementary Figure 11), we observe that *Dpt*-RFP expression is primarily localized in the anterior midgut and likely in the beginning of acidic region in larvae infected with Bt, Ecc and Lp.

> *Using TrpA1 and Dh31 mutants, the authors found both Ecc15 and Bt in the posterior midgut. Why are they not evenly distributed along the gut?*

We observe that bacteria are not evenly distributed along the gut in wild-type larvae as well, with LP. This suggests that the transit time in the anterior part of the gut may be relatively short due to active peristaltism, which would make this region function as a "checkpoint" for bacteria that are not supposed to be blocked. Indeed, we confirmed that peristaltism is active during our intoxication experiments, which could explain the rapid movement of bacteria through the anterior midgut.

In contrast, bacteria tend to remain longer in the posterior midgut, which corresponds to the absorptive functions of intestinal cells in this region. This would explain why we observe more bacteria in the posterior midgut for *Lp* in control larvae and for *Ecc15* and *Bt* in the

TrpA1- and Dh31- mutants. Although a few bacteria are still found in the anterior midgut, they are consistently in much lower numbers compared to the posterior, as shown in Figures 1A and 3A of our manuscript.

> *Last but not least, does the ROS/TrpA1/Dh31 axis affect AMP expression?*

We investigated whether the ROS/TrpA1/Dh31 axis influences AMP expression by performing RT-qPCR on the whole gut of larvae in wild-type, TrpA1-, and Dh31- genetic backgrounds. Larvae were fed with Lp, Ecc, Bt, or yeast (new data: Supplementary Figure 6). We monitored the expression of three different AMP-encoding genes and found that while AMP expression varied depending on the food content, there were no significant differences in AMP expression between the different genotypes.

Additionally, we provide imaging data from AMP reporter larvae (*pDpt*-Cherry) fed with fluorescent Lp or Bt (new data: Supplementary Figure 11). These results further confirm that the ROS/TrpA1/Dh31 axis does not significantly affect AMP expression in our experimental conditions.

> *(4) The TARM structure part is quite interesting. However, the authors did not show its relevance in their model. Is this structure the key-driven force for the blocking phenotype and killing phenotype?*

We agree that the TARM structures are a fascinating aspect of this study and acknowledge the interest in their potential role in the blocking and killing phenotypes. While we are keen to explore the specific contributions of these structures during bacterial intoxication, the current genetic tools available for manipulating TARMs target both TARM T1 and T2 simultaneously, as demonstrated by Bataillé et al., 2020 (Fig. 2). Of note, these muscles are essential for proper gut positioning in larvae, and their absence leads to significant defects in food intake and transit, which would confound the results of our intoxication experiments (see Fig. 6 from Bataillé et al., 2020).

Therefore, while TARMs are likely involved in these processes, the current limitations in selectively targeting them prevent us from definitively testing their role in bacterial blocking and killing at this stage. We hope to address this in future studies as more refined genetic tools become available.

> *Is the ROS/TrpA1/Dh31 axis required to form this structure?*

To determine whether the ROS/TrpA1/Dh31 axis is required for the formation of TARM structures, we examined larval guts from control, TrpA1-, and Dh31- mutant backgrounds. Our new data (Supplementary Figure 8) show that the TARM T2 structures are still present in the mutants, indicating that the formation of these structures does not depend on the ROS/TrpA1/Dh31 axis.

> ***Reviewer #2 (Public Review):***
>
> *This article describes a novel mechanism of host defense in the gut of Drosophila larvae. Pathogenic bacteria trigger the activation of a valve that blocks them in the anterior midgut where they are subjected to the action of antimicrobial peptides. In contrast, beneficial symbiotic bacteria do not activate the contraction of this sphincter, and can access the posterior midgut, a compartment more favorable to bacterial growth.*
>
> *Strengths:*
>
> *The authors decipher the underlying mechanism of sphincter contraction, revealing that ROS production by Duox activates the release of DH31 by enteroendocrine cells that*

> *stimulate visceral muscle contractions. The use of mutations affecting the Imd pathway or lacking antimicrobial peptides reveals their contribution to pathogen elimination in the anterior midgut.*
>
> *Weaknesses:*
>
> *The mechanism allowing the discrimination between commensal and pathogenic bacteria remains unclear.*

Based on our findings, we hypothesize that ROS play a crucial role in this discrimination process, with uracil release by pathogenic or opportunistic bacteria potentially serving as a key signal.

To test whether uracil could trigger this discrimination, we conducted experiments where Lp was supplemented with uracil. However, our results show that uracil supplementation alone was not sufficient to induce the blockage response (new data: Supplementary Figure 5). This suggests that while uracil may be a factor in bacterial discrimination, it is likely not the sole trigger, and additional bacterial factors or signals may be required to activate the blockage mechanism.

> *The use of only two pathogens and one symbiotic species may not be sufficient to draw a conclusion on the difference in treatment between pathogenic and symbiotic species.*

To address this concern, we performed additional intoxication experiments using *Escherichia coli* OP50, a bacterium considered innocuous and commonly used as a standard food source for *C. elegans* in laboratory settings. The results, presented in our updated data (new data: Fig 1B), show that *E. coli* OP50, despite being from the same genus as Ecc, does not trigger the blockage response. This further supports our conclusion that the gut's discriminatory mechanism is specific to pathogenic bacteria, and not merely based on bacterial genus.

> *We can also wonder how the process of sphincter contraction is affected by the procedure used in this study, where larvae are starved. Does the sphincter contraction occur in continuous feeding conditions? Since larvae are continuously feeding, is this process physiologically relevant?*

In our intoxication protocol, the larvae are exposed to contaminated food for 1 hour, during which the blockage ratio is quantified. Since this period involves continuous feeding with the contaminated food, we do not consider the larvae starved during the quantification process. Our observations show differences in the blockage response depending on the bacterial contaminant and the genetic background of the host. Additionally, we were able to trigger the blocking phenomenon using exogenous hCGRP.

Regarding the experimental setup for movie observations, it is true that larvae are immobilized on tape in a humid chamber, which is not a fully physiological context. However, in the new movie we provide (Movie 3), co-treatment with fluorescent Dextran (Red) and fluorescent Bt (Green) shows that both are initially blocked, followed by the posterior release of Dextran once the bacterial clearance begins.

Furthermore, to address the question of continuous exposure, we extended the exposure period to 20 hours instead of 1 hour. Even after prolonged exposure, we observed that pathogens are still blocked in the anterior part of the gut (new data: Supplementary Figure 2B). This supports the physiological relevance of the sphincter contraction and its ability to function under continuous feeding conditions.

> ***Reviewer #1 (Recommendations For The Authors):***
>
> *(1) The authors performed the experiments on Drosophila larvae. I wonder whether this model could extend to adult flies since they have shown that the ROS/TRPA1/Dh31 axis is important for gut muscle contraction in adult flies. If not, how would the authors explain the discrepancy between larvae and adults?*

We link the adult phenotype to the one we describe in larvae in order to have the candidate approach toward the ROS/TrpA1/Dh31 axis. As we already mention in the discussion, while larvae stay in the food, adult flies can go away. If larvae eject their gut content, they may ingest it within minutes. We clarify our idea in the last part of the discussion.

> *(2) The authors performed their experiments and proposed the models based on two pathogenic bacteria and one commensal bacterial at a relatively high bacterial dose. They showed that feeding Bt at 2X1010 or Ecc15 at 4X108 did not induce a blockage phenotype.*
>
> *I wonder whether larvae die under conditions of enteric infection with low concentrations of pathogenic bacteria.*

Video provided with Bt-GFP 1.3 10^10 CFU/mL (new data: Movie 5). When larvae eat less, there is no blockage and bacteria can reach the posterior midgut. Note that the fluorescence is weak due to the low amount of bacteria ingested. The movie shows an excretion of the bacteria. There is also no death of the larvae. Together these results suggest that below a given threshold, the virulence of the bacteria is too weak to i) trigger a blockage and 2/ kill the larva. The bacteria are likely eliminated through classical peristaltism.

> *If larvae do not show mortality, what is the mechanism for resisting low concentrations of pathogenic bacteria?*

Maybe we are below the threshold of virulence. See our response just above.

> *Why is this model only applied to high-dose infections?*

As mentioned in the manuscript, lower concentrations do not trigger the blockage and for lower concentrations with a GFP signal still detectable, wild-type animals resist the presence of live-bacteria within the posterior part of the intestine.

About the doses, the CFU should be considered. Indeed, there are around 5.10^4 CFU per midgut. In our experimental procedure we calculate the amount of bacteria for 500 µl of contaminated medium (i.e. 4.10^10 CFU/500µl of medium). Then around 50 larvae were deposited in the 500µl of contaminated media. In this condition, one larva ingests 5.10^4 CFU. Moreover, larvae are only fed for 1h.

So 1/ continuous feeding may also trigger locking even at lower doses and 2/ the other mechanisms of defenses (such as ROS) or peristalsis may be sufficient to eliminate lower doses (i.e. 10^3 CFU or below). See the new movie 5 we provide with *Bt-GFP 1.3 10^10 CFU/mL*

> *(3) The authors claim that the lock of bacteria happens at 15 minutes while killing by AMPs happens 6-8 hours later.*

Our CFU data indicate that it's after 4 to 6 hours that the quantity of bacteria decreases. We fixed this in the text.

> *What happened during this period?*

ROS activity (bacteriostatic and bacteriolytic), IMD activation, AMP transcription, translation, secretion and bacteriostatic as well as bacteriolytic activity.

> *More importantly, is IMD activity induced in the anterior region of the larval gut in both Ecc15 and Bt infection at 6 hours after infection?*

We provide new data for larval whole gut RT-qPCR data in wt, TrpA1- and Dh31- genetic background fed with Lp or Ecc or Bt or yeast only (new data: SUPP6). We monitored 3 different AMP-encoding genes and found differences related to the food content, but no differences between genotypes. In addition, we provide images from AMP reporter animals (Dpt-Cherry) fed with fluorescent Lp or Bt (new data: SUPP11) showing that with Bt blocked in the anterior part of the intestine, the *dpt* gene is mainly induced in this area. Note that in the larva infected with Lp-GFP, the Dpt-Cherry reporter is weakly expressed in the anterior midgut. In the posterior midgut, the place where Lp-GFP is established, Dpt-Cherry is barely detectable. This observation is in line with the previous observation made by Bosco-Drayon et al., (2012) demonstrating the low level of AMP expression in the posterior midgut due to the expression of the IMD negative regulators such as *amidases* and *pirk*. In the larva infected with Bt-GFP, note the obvious expression of DptCherry in the anterior midgut colocalizing with the bacteria (new data: SUPP11).

> *Are they mostly expressed in the anterior midgut in both bacterial infections? Several papers have shown quite different IMD activity patterns in the Drosophila gut. Zhai et al. have shown that in adult Drosophila, IMD activity was mostly absent in the R2 region as indicated by dpt-lacZ. Vodovar et al. have shown that the expression of dpt-lacZ is observable in proventriculus while Pe is not in the same region. Tzou et al. showed that Ecc15 infection induced IMD activity in the anterior midgut 24 hours after infection.*

In ctrl animals fed Bt, Ecc and Lp we see Dpt-RFP in anterior midgut and likely in the beginning of acidic region. See the new data: SUPP11 images provided for the previous remark.

> *Using TrpA1 and Dh31 mutants, the authors found both Ecc15 and Bt in the posterior midgut. Why are they not evenly distributed along the gut?*

Same is true with Lp in wt; not evenly distributed. As if the transit time in the anterior part is very short due to peristaltism which would fit for a check point area if you're not supposed to be blocked. Indeed, peristaltism is active during our intoxications. Then, it stays longer in the posterior part, fitting with the absorptive skills of the intestinal cells in this area. With Lp in ctrl or Ecc and Bt in TrpA1- and Dh31- mutants, there are always a few in the anterior midgut but always much less compared to the posterior. See our figure 1A and 3A.

> *Last but not least, does the ROS/TrpA1/Dh31 axis affect AMP expression?*

We provide larval whole gut RT-qPCR data in wt, TrpA1- and Dh31- genetic background fed with Lp or Ecc or Bt or yeast only (new data: SUPP6). We monitored 3 different AMPencoding genes and found differences related to the food content, but no differences between genotypes. In addition, we provide images from AMP reporter animals (pDptCherry) fed with fluorescent Lp or Bt, (new data: SUPP11).

> *(4) The TARM structure part is quite interesting. However, the authors did not show its relevance in their model. Is this structure the key-driven force for the blocking phenotype and killing phenotype?*

Indeed, we would like to explore the roles of these structures and the putative requirement upon bacterial intoxication using some driver lines developed by the team that studied these muscles *in vivo*. However, the genetic tools currently available will target TARMsT1 and T2 at the same time. See Fig 2 form Bataillé et al, . 2020. Moreover, these TARMs are, at first, crucial for the correct positioning of the gut within the larvae and their absence lead to a global food intake and transit defect that will bias the outcomes of our intoxication protocol (see fig 6 from Bataillé et al,. 2020).

> *Is the ROS/TrpA1/Dh31 axis required to form this structure?*

We provide images of larval guts from ctrl, TrpA1 and Dh31 mutants demonstrating the presence of the TARMs T2 structures despite the mutations (new data: SUPP8). In addition, we provide representative movies of peristalsis in intestines of Dh31 mutants fed or not with Ecc to illustrate that muscular activity is not abolished (new data: Movie 9 and Movie 10).

> *Minor points:*
>
> *(1) Why not use the Pros-Gal4/UAS-Dh31 strain in Figure 3B in addition to hCGRP?*

We opted for exogenous hCGRP addition because it allowed us precise timing control over Dh31 activation. Overexpression of Dh31 from embryogenesis or early larval stages could have significant and unintended effects on intestinal physiology, potentially confounding the results. While temporal control using TubG80ts could be an alternative, our focus was on identifying the specific cells responsible for the phenomenon.

To achieve this, we perturbed Dh31 production via RNAi, specifically targeting a limited number of enteroendocrine cells (EECs) using the DJ752-Gal4 driver, as described by Lajeunesse et al., 2010. Our new data (Supplementary Figure 4) demonstrate that Dh31 expression in this subset of cells is indeed necessary for the blockage phenomenon.

> *(2) Section title (line 287) refers to mortality, but no mortality data is in the figure.*

We agree that the title referenced mortality, whereas no mortality data was presented in this section. We have updated the title to better reflect the data discussed in this part of the manuscript.

> *(3) It may be better to combine ROS-related contents in the same figure.*

While it is technically feasible to consolidate the ROS-related content into one figure, doing so would require splitting essential data, such as the *Gal4* controls for the RNAi assays and parts of the survival phenotype data. We believe that the current structure of the study, which first explores the molecular aspects of the phenomenon and then demonstrates its relevance to the animal's survival, provides a clearer and more logical flow. For these reasons, we prefer to maintain the current figure layout.

> ***Reviewer #2 (Recommendations For The Authors):***
>
> *Major recommendation*
>
> *(1) Other wild-type backgrounds should be added (including the w Drosdel background of the AMP14 deficient flies) to check the robustness of the phenotype.*

To address the concern regarding the robustness of the phenotype across different wildtype backgrounds, we have tested additional genetic backgrounds, including w1, the isogenized w1118 and Oregon animals.

The results (new data: Figure 1C) demonstrate that Lp is able to transit freely to the posterior part of the intestine in all backgrounds, while Ecc and Bt are blocked in the anterior part. These findings confirm the robustness of the phenotype across different wildtype strains.

> *(2) Although we recognize that this may be limited by the number of GFP-expressing species, other commensal and pathogenic bacteria should be tested in this assay (e.g. E. faecalis and Acetobacter).*

We performed new intoxication experiments using *Escherichia coli* OP50, a wellestablished innocuous bacterial strain. The data, presented in Figure 1B (new data), show that *E. coli* OP50, despite being from the same genus as Ecc, does not trigger the blockage response. This further supports our hypothesis that the blockage phenomenon is specific to pathogenic bacteria and not simply related to the bacterial genus.

> *(3) It is important to test whether sphincter closure also occurs in continuous feeding conditions. This does not mean repeating all the experiments but just shows that this mechanism can take place in conditions where larvae are kept in a vial with food.*

While the movies we provide involve larvae immobilized on tape in a humid chamber, which is not a fully physiological context, we now provide new data (Movie 3) showing that, after co-treatment with fluorescent Dextran (Red) and fluorescent Bt (Green), both substances are initially blocked in the anterior midgut. Later, the dextran is released posteriorly once bacterial clearance has begun.

Additionally, we extended the feeding period in our experiments from 1 hour to 20 hours to simulate more continuous exposure to contaminated food. Even under these prolonged conditions, we observed that pathogens are still blocked in the anterior part of the gut (new data: Supplementary Figure 2B). This confirms that the sphincter mechanism can function in continuous feeding conditions as well.

> *(4) What are the molecular determinants discriminating innocuous from pathogenic bacteria? Addressing this point will increase the impact of the article. The fact that Relish mutants have normal valve constriction suggests that peptidoglycan recognition is not involved. Is there a sensing of pathogen virulence factors?*

Our data suggest that uracil could be a key molecular determinant in discriminating between innocuous and pathogenic bacteria, as previously described by the W-J Lee team in several studies on adult *Drosophila*. However, in our experiments, exogenous uracil addition using the blue dye protocol (Keita et al., 2017) did not induce any significant changes in the larvae. Similarly, uracil supplementation in adult flies failed to trigger the *Ecc* expulsion and gut contraction phenotype, as reported by Benguettat et al., 2018.

To further investigate this, we tested the addition of uracil during Lp-GFP intoxication. In these experiments, we did not observe any blockage of *Lp* (new data: Supplementary Figure 5). These results suggest that uracil might not be the sole trigger for the blockage response, or we may not be providing uracil exogenously in the most effective way. Alternatively, there could be other pathogen-specific virulence factors that contribute to this discrimination mechanism.

> *To address this question, the authors should infect larvae with Ecc15 evf- mutants or Ecc15 lacking uracil production.*

Thank you for your suggestion to use *Ecc15* evf- mutants or *Ecc15* lacking uracil production to explore the role of uracil in bacterial discrimination. While we have provided some data

using uracil supplementation (new data: Supplementary Figure 5), we agree that testing mutants like *PyrE* would be an important next step. Unfortunately, we currently lack access to fluorescent *PyrE* or *Ecc15* evf- mutants.

We are planning to address this by developing a new protocol involving fluorescent beads alongside bacteria. This approach will allow us to test several bacterial strains in parallel and better define the size threshold of the valve. However, we do not have the relevant data yet, but this will be a key focus of our future work.

> *Similarly, does feeding heat-killed Ecc15 or Bt induce sequestration in the anterior midgut (larvae may be fed dextran-FITC at the same time to track bacteria)?*

Unfortunately, in our attempts to test heat-killed or ethanol-killed fluorescent *Ecc15* for these experiments, we encountered an issue: while we were able to efficiently kill the bacteria, we lost the GFP signal required to track their position in the gut. This made it challenging to assess whether sequestration in the anterior midgut occurs with non-viable bacteria.

> *Is uracil or Bt toxin feeding sufficient to induce valve closure?*

As previously mentioned, uracil is a strong candidate for bacterial discrimination, and we have tested its role by adding exogenous uracil during Lp-GFP intoxication. However, in these experiments, *Lp* was not blocked (new data: Supplementary Figure 5). This suggests that uracil alone may not be sufficient to induce valve closure, or it may not be the only factor involved. It is also possible that our method of exogenous uracil supplementation may not be effectively mimicking the endogenous conditions.

Regarding Bt, we used vegetative cells without Cry toxins in our experiments. Cry toxins are only produced during sporulation and are enclosed in crystals within the spore. The Bt strain we used, 4D22, has been deleted for the plasmids encoding Cry toxins. As a result, there were no Cry toxins present in the Bt-GFP vegetative cells used in our assays. This has been clarified in the Materials and Methods section of the manuscript.

> *Would Bleomycin induce the same phenotype?*

Indeed, Bleomycin, as well as paraquat, has been shown to damage the gut and trigger intestinal cell proliferation in adult *Drosophila* through mechanisms involving TrpA1. Testing whether Bleomycin induces a similar phenotype in larvae would indeed be interesting.

However, one challenge we face in our intoxication protocol is that larvae tend to stop feeding when chemicals are added to their food mixture. We encountered similar difficulties in our DTT experiments, which were challenging to set up for this reason. Consequently, we aim to avoid approaches that might impair the general feeding activity of the larvae, as it can significantly affect the outcomes of our experiments.

> *Could this process of sphincter closure be more related to food poisoning?*

If gut damage were the primary trigger for sphincter closure, we would indeed expect the blockage phenomenon to occur later following bacterial exposure. However, in our experiments, we observe the blockage occurring early after bacterial contact, suggesting that damage may not be the main trigger for this response.

That said, we have not yet tested bacterial mutants lacking toxins, nor have we tested a direct damaging agent such as Bleomycin, as proposed. These would be valuable future experiments to explore the potential role of gut damage more thoroughly in this process.

> *(5) Is Imd activation normal in trpA1 and DH31 mutants? The authors could use a diptericin reporter gene to check if Diptericin is affected by a lack of valve closure in trpA1.*

To address this, we performed RT-qPCR on whole larval guts from wt, TrpA11 and Dh31KG09001 genetic background. Larvae were fed with Lp, Ecc, Bt or yeast only (new data: SUPP6). We monitored the expression of three different AMP-encoding genes and found that while AMP expression varied depending on the food content, there were no significant differences in AMP expression between the genotypes.

Additionally, we provide imaging data from AMP reporter animals (*pDpt*-Cherry) in a wildtype background, fed with fluorescent Lp or Bt (new data: Supplementary Figure 11). These images also support the conclusion that *Diptericin* expression is not significantly affected by a lack of valve closure in *trpA1* and *Dh31* mutants.

> *(6) Are the 2-6 DH31 positive cells the same cells described by Zaidman et al., Developmental and Comparative Immunology 36 (2012) 638-647.*

The cells identified as hemocytes in the midgut junctions by Zaidman et al. are likely the same cells we describe in our study, as they are located in the same region and are *Dh31* positive. We have added a reference to this paper and included lines in the manuscript acknowledging this connection.

Although confirming whether these cells are *Hml*+, *Dh31*+, and *TrpA1*+ would clarify their exact identity, this falls outside the scope of our current study. However, the possibility that these cells play a role in physical barrier immunity and also possess a hemocyte identity is indeed intriguing, and we hope future research will explore this further.

> *Minor points*
>
> *(1) The mutations should be appropriately labelled with the allele name.*

This has been fixed in the main text, in Fig Legends, and in figures.

> *(2) Line 230-231: the sentence is unclear to me.*

We simplified the sentence and do not refer to the expulsion in larvae.

> *(3) Discussion: although the discussion is already a bit long, it would be interesting to see if this process is likely to happen/has been described in other insects (mosquito, Bactrocera, ...).*

We reviewed the available literature but were unable to find specific examples describing the blockage phenomenon in other insects. Most studies we found focused on symbiotic bacteria rather than pathogenic or opportunistic bacteria. However, as mentioned in our manuscript, the anterior localization of opportunistic or pathogenic bacteria has been observed in *Drosophila* by independent research groups.

> *(4) Line 546: add the Caudal Won-Jae Lee paper to state the posterior midgut is less microbicidal.*

We added the reference at the right place, mentioning as well that it concerns adults.

> *(5) Figure 6 indicates what the cells are, shown by the arrow.*

The sentence ‘the arrows point to TARMs’ is present in the legend of Fig6.

> *(6) Does the sphincter closure depend on hemocytes?*

As mentioned above, the cells we identify as *TrpA1+* in the midgut junction may be the same cells described by Zaidman et al., 2012, and earlier by Lajeunesse et al., 2010. Inactivating hemocytes using the *Hml-Gal4* driver may also affect these *Dh31+* cells, as they share similarities with hemocytes, as pointed out by Zaidman et al. However, distinguishing between hemocytes and *Dh31+*/*TrpA1+* cells would require a genetic intersectional approach, which is beyond the scope of our current study.

Nevertheless, the possibility that these cells play a dual role in immunity (through blockage) and share characteristics with hemocytes while functioning as enteroendocrine cells (EECs) is quite intriguing and deserves further exploration in future studies.

https://doi.org/10.7554/eLife.98716.2.sa0